

1991

Processing and microstructure development of YB₂ Cu₃ O_{6+x} ceramic superconductors

Lijie Zhang
Lehigh University

Follow this and additional works at: <https://preserve.lehigh.edu/etd>

 Part of the [Materials Science and Engineering Commons](#)

Recommended Citation

Zhang, Lijie, "Processing and microstructure development of YB₂ Cu₃ O_{6+x} ceramic superconductors" (1991). *Theses and Dissertations*. 5429.
<https://preserve.lehigh.edu/etd/5429>

This Thesis is brought to you for free and open access by Lehigh Preserve. It has been accepted for inclusion in Theses and Dissertations by an authorized administrator of Lehigh Preserve. For more information, please contact preserve@lehigh.edu.

Processing and Microstructure Development of
 $\text{YBa}_2\text{Cu}_3\text{O}_{6+x}$ Ceramic Superconductors

by

Lijie Zhang

A Thesis
Presented to the Graduate Committee
of Lehigh University
in Candidacy for the Degree of
Master of Science
in
Materials Science and Engineering

Lehigh University

1990

Certificate of Approval

This thesis is accepted and approved by the Department of Materials Science and Engineering in partial fulfillment of the requirements for the Degree of Master of Science.

12/4/90
Date

Helen Chan

Martin P. Harmer
Professors in Charge

Richard W. Hefner
Department Chairperson

Acknowledgements

I would like to thank my advisors Dr. Helen M. Chan and Dr. Martin P. Harmer for guidance throughout the course of this research.

I also acknowledge all those who have made contributions. The financial support from the Lehigh University Consortium for Superconducting Ceramics (LUCSC), of which Dr. D. M. Smyth is Chairman, is graciously appreciated.

TABLE OF CONTENTS

	Page
Title page	i
Certificate of Approval	ii
Acknowledgements	iii
Table of Contents	iv
List of Figures	v
List of Tables	vii
Abstract	1
1. Introduction and Background	2
1.1 Overview	3
1.2 Y-Ba-Cu-O System	4
1.2.1 Phase Transformation and Superconducting Phase Microstructure	4
1.2.2 Bulk Samples	8
1.2.3 Introducing Texture to Improve J_c	9
2. Experimental Procedure	11
2.1 Preparation of Powder and Bulk Samples	11
2.2 In-situ Annealing Studies	13
2.3 Sintering and Melt Processing	13
2.3.1 Single-step Thermal Treatment	13
2.3.2 Quench Experiments	14
2.3.3 Two-step Thermal Treatment	17
2.4 Seeding-induced Aligned Microstructure	20
3. Results and Discussion	21
3.1 In-Situ Annealing Studies	21
3.2 Influence of Thermal Processing on Texture Formation	30
3.2.1 One-step Thermal Treatment	30
3.2.2 Quench Experiments	33
3.2.3 Two-Step Thermal Treatment	38
3.3 Texture by Seeding	43
4 Summary and Conclusions	46
References	47
Vita	52

List of Figures

Number	Page
1. The orthorhombic crystal structure of yttrium barium cuprate.	7
2. Flow chart of powder preparation.	12
3. Schematic diagram of quenching experiments.	16
4. Schematic diagram of two kinds of thermal treatment.	18
5. SEM photograph showing a grain-boundary second phase in a $\text{YBa}_2\text{Cu}_3\text{O}_{6+x}$ sample heated to 700°C in the optical hot-stage.	22
6. X-ray maps showing the relative variation in Carbon, Barium, Yttrium, Copper, and Oxygen Contents between the matrix and the second phase. The conventional secondary electron image is shown in (a).	23
7. Comparison of voltage versus current density curves for $\text{YBa}_2\text{Cu}_3\text{O}_{6+x}$ specimens: (1) air annealed for 2 hr at 800°C and (2) oxygen annealed for 10 hr at 800°C . Both samples were subsequently annealed in flowing oxygen at 500°C for 20 hr (77K, zero magnetic field).	26
8. SEM photograph showing an indentation site in a $\text{YBa}_2\text{Cu}_3\text{O}_{6+x}$ specimen immersed 12 hr in ethanol and annealed 2 hr at 800°C in air.	27
9. SEM photograph showing a $\text{YBa}_2\text{Cu}_3\text{O}_{6+x}$ sample surface covered with Ba-C-O second phase. Sample annealed 2 hr at 800°C in CO_2 .	29
10. SEM micrograph showing (A) conventional sintered $\text{YBa}_2\text{Cu}_3\text{O}_{6+x}$ microstructure, sintered 20 hr at 920°C ; (B) aligned regions in $\text{YBa}_2\text{Cu}_3\text{O}_{6+x}$ sample sintered 0.5 hrs at 1050°C , in O_2 ; second phases indicated by arrows a: 211 phase, b: Cu-rich phase, and c: Ba-rich phase.	32
11. Section through $\text{BaO} \cdot \text{Y}_2\text{O}_3 \cdot \text{CuO}$ phase diagram.	35
12. SEM micrographs of samples quenched during heating stage. Quench temperature from A: 950°C , B: 970°C , C: 990°C D: 1010°C , E: 1030°C , F: 1050°C . Note absence of grain alignment.	36

- | | | |
|-----|--|----|
| 13. | SEM micrograph of sample quenching from 900°C during the cooling stage, second phases depicted by arrows a: 211 phase, b: CuO. | 37 |
| 14. | Optical micrograph of 123 sample after thermal step treatment (1050°C/970°C, second stage hold time H ₂ =5 hrs, in O ₂). Domain is > 2mm in size. | 39 |
| 15. | Optical micrograph of two-step heat treatment sample (1050°C/970°C, H ₂ =5 hrs, in O ₂) by polaroid. Twinning within the grains is clearly evident. The second phase particles are 211. | 40 |
| 16. | Optical micrograph of YBa ₂ Cu ₃ O _{6+x} sample after thermal step treatment (1050°C/970°C, H ₂ =5 hrs, in O ₂) showing impurities between domains. | 42 |
| 17. | Optical micrograph of seeded 123 specimen showing
a, regions (1mm) of highly aligned grains,
b, within aligned domain, second phase particles of 211. | 44 |
| 18. | Current density for seeded 123 specimens, sintered at 1010°C, 1/2 hr, in O ₂ . | 45 |

List of Tables

Number

Page

1. Experimental data of thermal step treatments. 19
2. Results of chemical analysis using X-ray Wavelength Dispersive Spectroscopy. 24

ABSTRACT

Superconducting $\text{YBa}_2\text{Cu}_3\text{O}_{6+x}$ was found to be very sensitive to the atmosphere during thermal treatment. During annealing in air at temperatures above 450°C , localized melting occurred, and second phases near the grain boundaries were observed using optical hot-stage microscopy. Quantitative chemical analysis using wavelength dispersive spectroscopy (WDS) indicated that the second phase was composed of a barium oxycarbonate. The source of carbon in the second phase was identified to be CO_2 from the atmosphere. The formation of the second-phase during CO_2 -annealing was not reversible by re-annealing in pure oxygen.

A texture study, using a melt-processing technique, was carried out with the aim of improving critical current density. The microstructure and properties of the samples were found to be very sensitive to the heat treatment. Variables such as sintering temperature, holding time and cooling rate were studied. A series of heat treatment experiments was performed in order to study grain alignment. Quenching tests with temperatures ranging from 950°C to 1050°C indicated that the volume fraction of second phases increased as the quenching temperature was increased. The second phases strongly reacted with the aqueous medium during polishing, and they were unstable at room temperature.

Aligned microstructures were obtained by heating $\text{YBa}_2\text{Cu}_3\text{O}_{6+x}$ above the peritectic temperature ($T_p=1002^\circ\text{C}$), followed by slow cooling. This process yielded aligned regions of approximately 200 microns in size. The degree of alignment was enhanced by seeding, where inclusions of aligned grains were added to the starting powders. For these samples aligned regions were obtained greater than 1 mm in size. Another method found to increase the degree of alignment was that of dual stage heat treatments; in this case aligned regions 2 mm were obtained. The critical current density of the aligned samples increased by one order of magnitude compared with the normal sintered samples.

1 INTRODUCTION AND BACKGROUND

The recently developed ceramic superconductors lose their electrical resistance at the high transition temperature [1], and could lead to incredible savings in energy. Commercial applications of superconductors include energy storage, magnetic levitation, electric power generators, and electric power transmission systems. For instance, they could be used to produce small but more powerful computers. Intense magnetic fields can be generated by the superconductors leading to the development of a superfast, magnetically levitated train. Superconducting power lines transmit electricity without loss of power and the electric energy can be stored indefinitely as a circulating current [2].

In 1986, a new unusual class of ceramic compounds of high T_c superconductors was discovered [3]. These new ceramic materials required cooling only to 90K to become superconductors [1]. The transition temperature is greatly increased over conventional superconductors, and inexpensive liquid nitrogen can be used as a coolant (77K), which could bring superconductivity into practical applications.

One of the high T_c superconducting compounds is $YBa_2Cu_3O_{6+x}$, and an extensive amount of research has been done on this material. There are, however, many processing-related problems associated with it. For instance, it is difficult to obtain sintered densities above 95% theoretical density. Also the critical current density (J_c) of the bulk polycrystalline samples is much lower than that for the single crystal samples (about four orders of magnitude) which impedes its use in practical applications. Likely causes of a grain-boundary barrier to current flow include microcracking, due to thermal or transformation stresses, segregation of impurities to grain boundaries, and the

presence of a non-superconducting layer or phase at grain boundaries, which may be amorphous and different in composition from the bulk. In addition, for bulk samples, a high-misorientation angle grain boundary restricts the transport of current across the grain boundary [4]. Bulk samples of sintered $\text{YBa}_2\text{Cu}_3\text{O}_{6+x}$ are not stable for long periods of time in air, and they strongly react with water to form other phases, which destroy the superconducting properties [5]. Superconducting $\text{YBa}_2\text{Cu}_3\text{O}_{6+x}$ is very sensitive to the sintering temperature, cooling rate [6], sintering atmosphere and annealing temperature [7]. Carbon contamination is another problem, which is largely an environmental artifact. It is relatively easy to detect carbon segregation at grain boundaries by Auger microscopy [8]. However, studies have shown that grain-oriented bulk samples have great potential for enhancing J_c [9-11]. Obviously there is a need for investigation of these areas. This thesis explores several areas of the microstructure development of $\text{YBa}_2\text{Cu}_3\text{O}_{6+x}$, with emphasis on the effect of processing variables on the formation of non-superconducting second phases and development of grain alignment.

1.1 Overview

Superconductivity is a phenomenon in which the electrical resistivity drops to “zero” suddenly at the transition temperature, T_c . Since Dutch physicist Heike Kamerlingh Onnes discovered superconductivity in mercury in 1911, the discovery of new materials has been responsible for T_c rising at a steady value of about 4 degrees Kelvin per decade [1]. A superconducting material is perfectly diamagnetic and therefore expels magnetic

flux. In order to remain superconducting, superconductors must be kept at a condition where the surface current density is below the critical current density (J_c) and the total magnetic field strength is lower than the critical field (H_c).

In 1986, a breakthrough occurred when Bednorz and Muller discovered a new class of ceramic compounds containing Ba-La-Cu-O that showed superconductivity at 35K [12]. This T_c is much higher than the conventional superconductors. Other researchers subsequently found other high T_c superconducting systems, such as Y-Ba-Cu-O (T_c :90K) [13], Bi-Ca-Sr-Cu-O (T_c :85K-110K) [14], and Tl-Ca-Ba-Cu-O (T_c :100K-125K) [15] systems. Because of the higher T_c values for these systems, liquid nitrogen (boiling temperature 77K) can be used to keep the materials in the superconducting state, rather than expensive liquid helium. Consequently, these materials have potential for practical applications.

1.2 Y-Ba-Cu-O System

Most of the research on ceramic superconductors has been done on the Y-Ba-Cu-O system (including this thesis), and so the discussion will be limited to this compound.

1.2.1. Phase Transformation and Superconducting Phase Microstructure

The superconducting phase of $YBa_2Cu_3O_{6+x}$ has an orthorhombic crystal structure with ordered oxygen vacancies. Its structure is oxygen deficient relative to the ideal perovskite structure [16,17]. The unit cell is such that b is slightly larger than a . The

oxygen atoms are ordered in the basal plane (Cu-O plane) of the structure, as shown in Figure 1. The lattice parameters are $a=3.82\text{\AA}$, $b=3.88\text{\AA}$, $c=3.68\text{\AA}$.

On cooling from the sintering temperature, the structure undergoes a phase transformation within the range $0 < x < 1$ from tetragonal to orthorhombic, which is dependent on oxygen partial pressure and temperature [18-24]. The tetragonal phase is non-superconducting with disordered oxygen vacancies. At the sintering temperature, usually above 900°C , the tetragonal structure dominates. To obtain the superconducting orthorhombic structure, oxygen annealing in which oxygen re-enters the $\text{YBa}_2\text{Cu}_3\text{O}_{6+x}$ structure is necessary. Oxygen annealing is usually carried out in a pure oxygen atmosphere at a temperature range of 400°C to 600°C [25-27]. The required oxidation time depends on the specimen size and density. Usually, above 20 hours is required because oxygen diffusion is slow. As the tetragonal-orthorhombic phase transformation proceeds, a volume change takes place in the unit cell due to the oxygen ordering along the b axis [28]. There is a twin structure in $\text{YBa}_2\text{Cu}_3\text{O}_{6+x}$, which has been associated with the switching of Cu-O and Cu-V (vacancy) chains across the twin boundary [29-31]. When the oxygens order in the basal copper plane, elongation of the b axis and contraction of the a axis occur. A shear stress is created when the a-b plane changes from a square to a rectangle. To accommodate the volume stress, the lattice structure must deform plastically so that the energy of the system is lowered. As a result of the transformation, twins are formed [32]. At the twin boundary, the oxygen and oxygen vacancies redistribute to minimize the free energy in the orthorhombic phase. The tetragonal-orthorhombic phase transformation in $\text{YBa}_2\text{Cu}_3\text{O}_{6+x}$ is an oxygen diffusion controlled isothermal shear transformation [33-34]. A shear transformation usually forms shear bands, which are located at the grain boundaries in $\text{YBa}_2\text{Cu}_3\text{O}_{6+x}$ and cause highly stressed regions. The stressed regions are sensitive to

an externally applied magnetic field because of their low T_c and H_{c2} (critical magnetic field) values and thus are responsible for weak links [35]. At the twin boundaries the cell edge with the enhanced oxygen content switches from one cell edge to the other, effectively rotating the unit cell through almost 90° . The two orientations share a common (110) plane in the twin boundary [36].

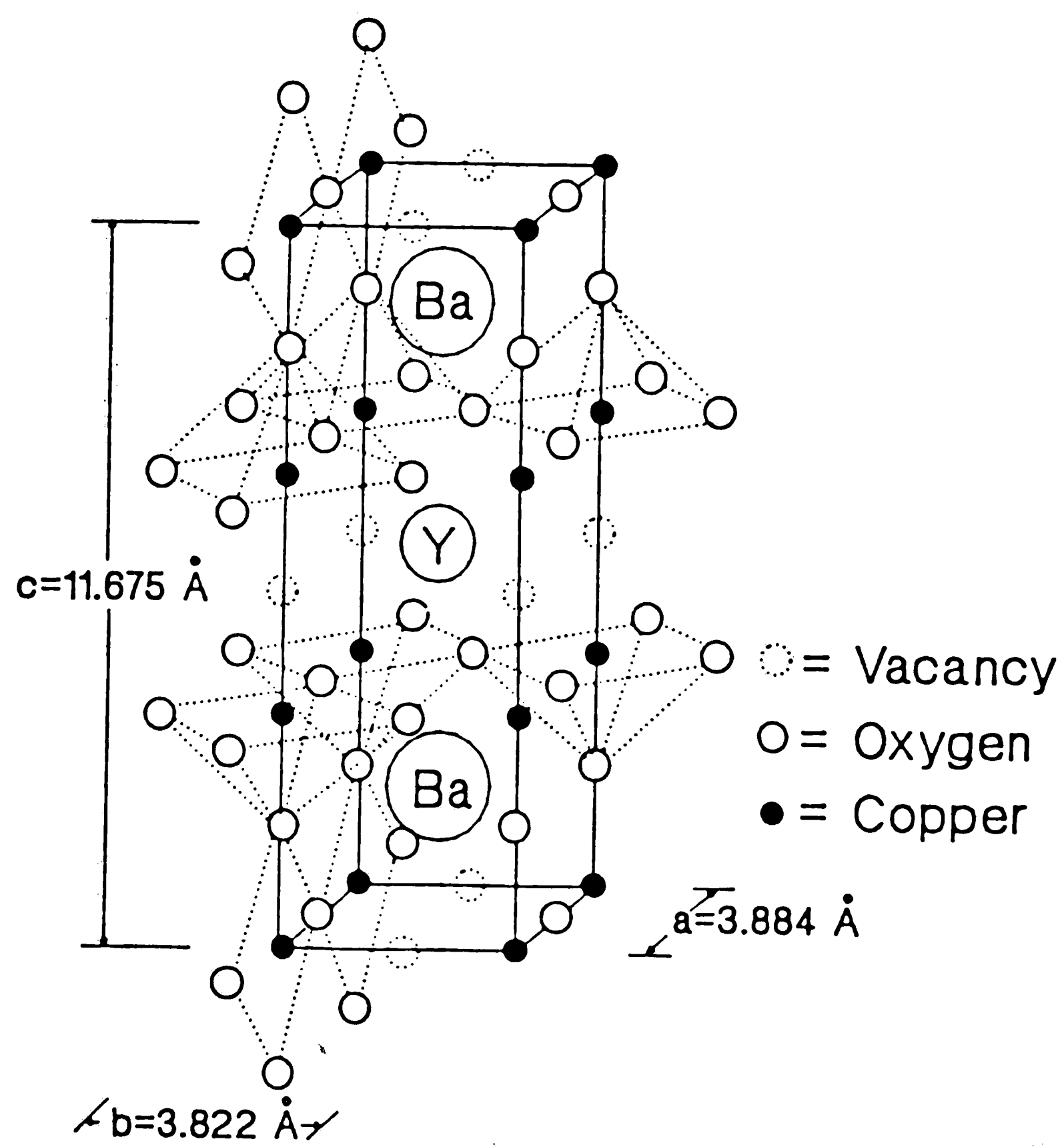


Fig. 1 The orthorhombic crystal structure of the yttrium barium cuprate.

1.2.2 Bulk Samples

The transport critical current density (J_c) in $\text{YBa}_2\text{Cu}_3\text{O}_{6+x}$ polycrystalline samples is very low, with values on the order of $10\text{-}100 \text{ A/cm}^2$ at 77K in zero magnetic field [37], while most commercial applications require J_c to be greater than 10^5 A/cm^2 . However, single crystals of $\text{YBa}_2\text{Cu}_3\text{O}_{6+x}$ have been shown to exhibit a transport J_c in excess of 10^5 A/cm^2 at 77K [38]. This disparity is attributed to the presence of randomly-oriented grain boundaries, second phases, pores and microcracks in bulk polycrystalline samples.

Numerous investigations have implicated grain boundaries as the cause of the low critical current densities in bulk samples [39,40]. There are non-superconducting second phases present at many of the grain boundaries. These regions could be semiconducting or insulating layers. The presence of these second phases causes the grain boundaries to act as superconducting-normal-superconducting junctions. Even for normally "clean" grain boundaries, the low J_c in bulk materials may be the result of inefficient transport between randomly oriented neighboring grains (crystal orientation change) due to intrinsic anisotropic conduction [42]. Another possibility for low J_c is the occurrence of microcracking due to thermal expansion anisotropy along the a-axis and c-axis [41]. Microcracks can often be observed along grain boundaries which are parallel to the basal plane. When the sample is cooled down from the sintering temperature, the dimensional change normal to the basal plane (along c-axis) is much larger than the change parallel to the basal plane; As a result, microcracking may occur.

In bulk materials, other problems result from the reaction of $\text{YBa}_2\text{Cu}_3\text{O}_{6+x}$ with the environment. The degradation of $\text{YBa}_2\text{Cu}_3\text{O}_{6+x}$ superconducting oxide ceramics can be related to environmental effects, e.g. corrosion by water, or to aging effects due to long-

term electrical loads or thermal cycling. In a study by Fitch et al. [43], the bulk density of corroded bars decreased with increasing corrosion time. The superconducting phase is deteriorated when exposed to humid ambient for long periods of time [44-46]. Second phases are formed similar to those formed from thermal treatment in air [47].

There are several possibilities for optimizing the transport J_c in bulk polycrystalline samples. These include the following general methods: orient the grains, minimize the number of grain boundaries, increase the area for current transfer across the grain boundaries in the direction of current flow, and reduce impurities and/or non-high- T_c phases between grains.

1.2.3 Introducing Texture to Improve J_c

The $YBa_2Cu_3O_{6+x}$ superconductor has a strongly anisotropic conductivity [42]. Structural analysis has shown that there are one-dimensional Cu-O chains as well as two-dimensional Cu-O planes in the $YBa_2Cu_3O_{6+x}$ structure. Both one-dimensional and two-dimensional features may be making contributions to the high-transition-temperature superconductivity [48]. Since the conductivity is anisotropic, it is thought that aligning the grain boundaries should allow the current to flow along an unobstructed path.

There are several different ways of introducing a pronounced texture in the bulk polycrystalline $YBa_2Cu_3O_{6+x}$ superconductor. For instance, sinter-forging was used to achieve crystallographic orientation in $YBa_2Cu_3O_{6+x}$, and the c-axis tended to be aligned parallel to the applied stress direction [49]; magnetic field alignment utilizes the anisotropic magnetic susceptibility [50], and deformation texture uses the anisotropic fracture behavior [51]. Substrate-induced texture has been performed, using epitaxial

growth of the superconductor on a suitable substrate material [52]. Melt-texturing [53] involves melting of the $\text{YBa}_2\text{Cu}_3\text{O}_{6+x}$ into a complete or partial liquid state and then directionally regrowing the superconducting crystals in the presence of a temperature gradient. And other researchers [54,55] obtained an aligned microstructure, involving no temperature gradient.

The crystallographic alignment eliminates the anisotropy-originated weak connection at high-angle grain boundaries [4]. Also microcrack formation near the grain boundaries, arising from severe thermal contraction anisotropy and the tetragonal-orthorhombic transformation, is minimized. The continuously growing crystal fronts of the superconducting phase during directional growth are likely to push away impurities (including carbonaceous compounds) to the side or front of the crystal, thus making them non- or less- interfering in supercurrent flow. Critical-current and lower-critical field measurements show that the $\text{YBa}_2\text{Cu}_3\text{O}_{6+x}$ superconductor is strongly anisotropic with the good conducting directions being along the Cu-O planes. Substantial increases in critical current density can be obtained by the production of highly textured microstructures in which the c axes of the grains are nearly parallel.

A high degree of grain alignment can increase the area for current transfer across the grain boundaries in the direction of current flow, if impurities between grains are reduced. Dimos et. al. [4] found that the critical current across a grain boundary decreased as the misorientation angle between the grains increased. For small misorientation angles, the ratio of the grain-boundary critical current density to the bulk critical current density was roughly proportional to the inverse of the misorientation angle. For large angles, this ratio saturated to a value of about 1/50. Many researchers have stated that grain alignment in 123 can dramatically improve J_c [55]. For instance, Jin [53] and his co-workers observed J_c values of $17000\text{A}/\text{cm}^2$ in 123 specimens which

contained highly aligned grains, fabricated by a melt texturing technique.

2 EXPERIMENTAL PROCEDURE

2.1 Preparation of Powder and Bulk Samples

$\text{YBa}_2\text{Cu}_3\text{O}_{6+x}$ superconducting powder was prepared using the conventional mixed oxide route. Dry Y_2O_3 , BaCO_3 , and CuO powders corresponding to a stoichiometric Y:Ba:Cu ratio of 1:2:3 were mixed by ball-milling for 12 hours in ethyl alcohol using zirconia grinding media. After drying, the mixture was calcined at 850°C in air over a period of 12 hours. After regrinding, a second calcination of the powders was carried out at 880°C in air for 12 hours. During this stage the powders became completely black in color, characteristic of the superconducting phase. X-ray diffraction results showed that the powder was single phase $\text{YBa}_2\text{Cu}_3\text{O}_{6+x}$. The recalcined powders were used to prepare pellets for sintering. Schematic details of this procedure are described in Fig.2.

Rectangular bar-shaped samples with dimensions 25x6x5 mm were made by cold uniaxial pressing of the recalcined powder at 26 ksi. The specimens were sintered in a box furnace at 930°C , for 20 hours in air. After furnace cooling down to 500°C , the sintered specimens were annealed in flowing oxygen for 20 hours at this temperature.

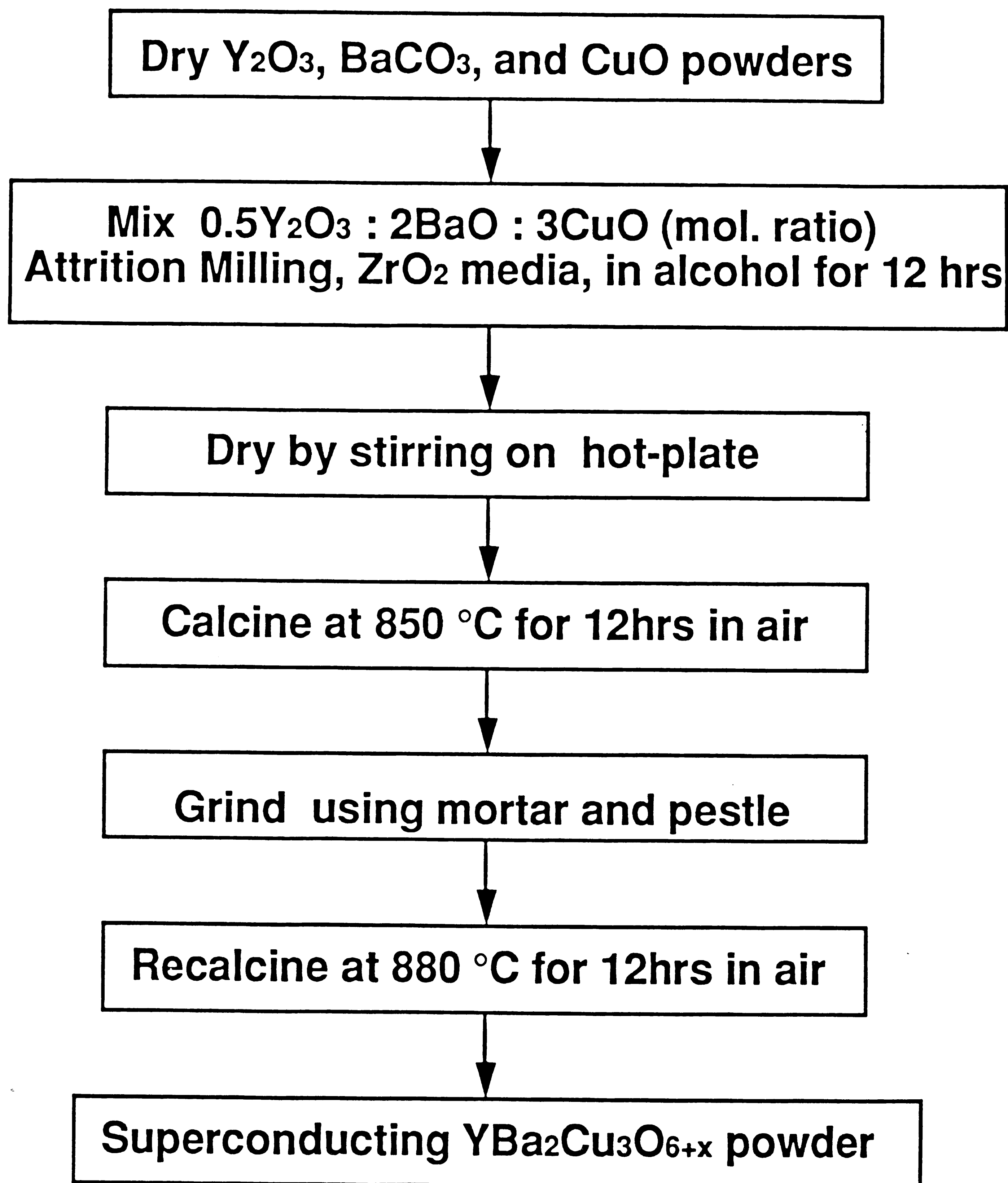


Fig. 2 Flow chart of powder preparation

2.2 In-situ Annealing Studies

In-situ annealing studies were performed on polished specimens by means of optical hot-stage microscopy. A series of samples was heated to temperatures ranging from 700°C to 950°C in air. The heating and cooling rates varied between 10°C/min to 50°C/min and were microprocessor-controlled. Microstructural changes were continuously recorded using video.

Polished specimens were annealed in a box furnace at 800°C, using atmospheres of flowing CO₂, O₂ and air. The purpose of these experiments was to assess the effect of various atmospheres on microstructure development. In order to analyze the formation of any second phases, the polished specimen was indented and then soaked in alcohol, which is a polishing lubricant. The specimen was then annealed for 2 hours at 800°C in air.

2.3 Sintering and Melt Processing

2.3.1 Single-step Thermal Treatment

For the texture development study, the specimens were heated at temperature close to the peritectic temperature (1002°C).

The following series of experiments was conducted in order to study the development of texture:

1) Variation of sintering temperature: 950°C, 970°C, 990°C, 1010°C, 1030°C, 1050°C, 1070°C, and 1100°C; heating rate of 8°C/min, cooling rate of 0.5°C/min and holding 2

hours were used for each sintering temperature.

2) Variation of sintering hold time: 0.5h, 2h, 4h, 6h, 8h, and 20h; with a heating rate of $8^{\circ}\text{C}/\text{min}$, heating up to 1050°C , and then cooling with a rate of $0.5^{\circ}\text{C}/\text{min}$.

3) Variation of cooling rate: $0.1^{\circ}\text{C}/\text{min}$, $0.5^{\circ}\text{C}/\text{min}$, $1^{\circ}\text{C}/\text{min}$, $2^{\circ}\text{C}/\text{min}$, and $4^{\circ}\text{C}/\text{min}$, with a heating rate of $8^{\circ}\text{C}/\text{min}$, heating up to 1050°C , holding a period of 0.5 hr.

All the above sintered samples were subsequently annealed in the oxygen atmosphere at 500°C , with a hold for 20 hours.

2.3.2 Quench Experiments

In order to determine how the microstructure develops during the course of the heat treatment, a series of quenching experiments was conducted, in which the heat-treatment was interrupted (at different stages) by rapidly cooling the specimen to room temperature. From the experiments described previously, a high degree of grain alignment was obtained when the samples were sintered at 1050°C with a heating rate of $8^{\circ}\text{C}/\text{min}$ over a period of 0.5 hours, cooling at a rate of $0.5^{\circ}\text{C}/\text{min}$ down to 800°C in oxygen atmosphere. So, quenched samples were made every 20°C from 950°C to 1050°C . This is depicted schematically in Fig.3.

In the first stage, with a heating rate of $8^{\circ}\text{C}/\text{min}$, samples were heated in an oxygen atmosphere to the quenching temperatures: 950°C , 970°C , 990°C , 1010°C , 1030°C , and 1050°C , and then pulled out of the furnace to room temperature.

In the cooling stage, samples were heated up to 1050°C , held for 0.5h in O_2 , and then cooled at a rate of $0.5^{\circ}\text{C}/\text{min}$ to various quench temperatures: 1050°C , 1030°C , 1010°C , 990°C , 970°C , and 950°C .

All the samples were polished and observed using Scanning Electron Microscopy (SEM)

and Energy-Dispersive X-Ray Spectroscopy (EDS).

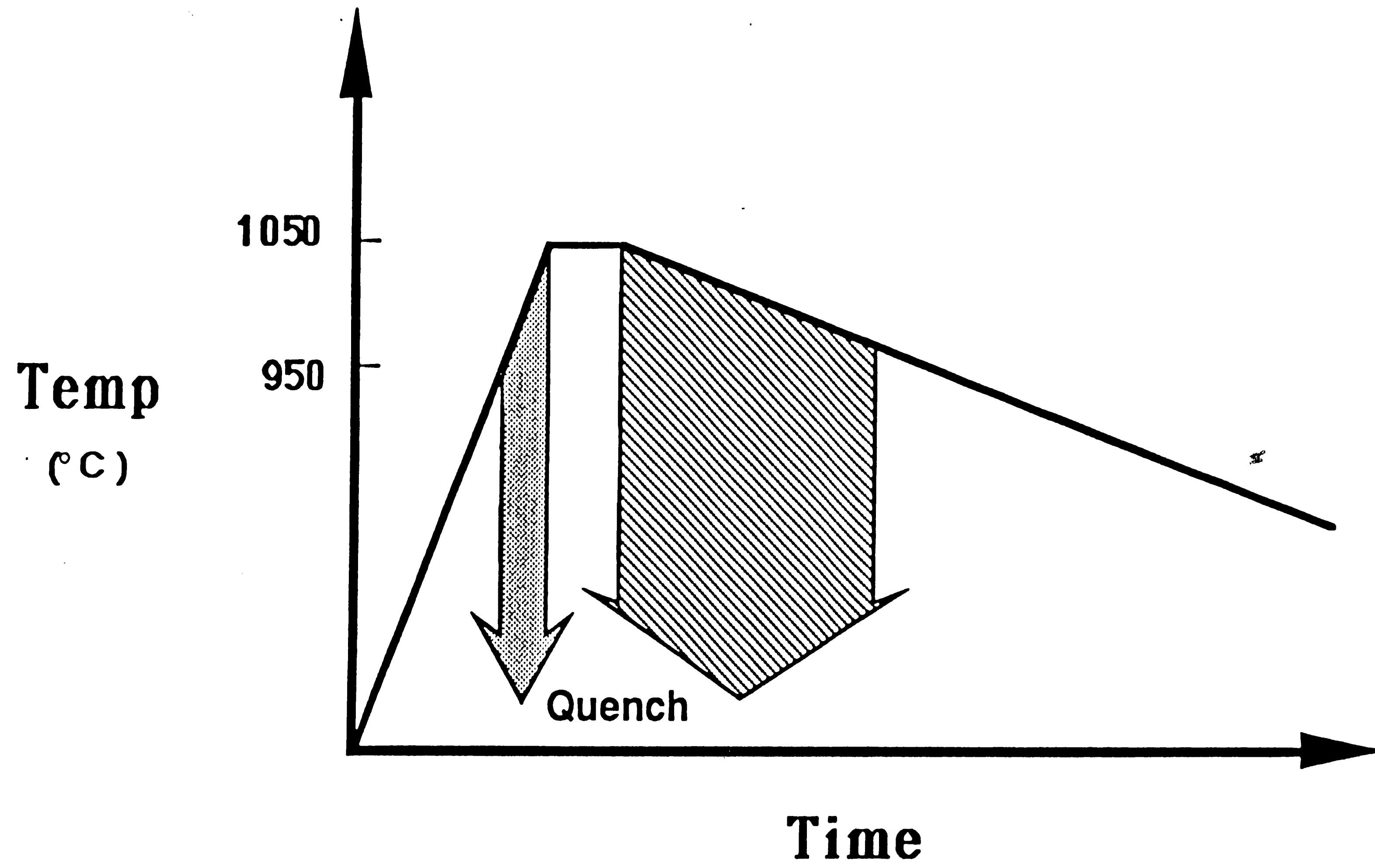


Fig.3 Schematic diagram of quenching experiments

2.3.3 Two-step Thermal Treatment

A two step thermal treatment was designed in order to provide sufficient time for the peritectic reaction to proceed to completion and form the 123 phase. The thermal step treatment technique is shown in Fig.4. The sample was held first at a temperature (T_1) which was slightly greater than the peritectic temperature. Following, they were cooled to a second temperature slightly below the peritectic temperature (T_2). It was used to produce an appreciable effective amount of liquid phase at T_1 , and offered a longer time for the peritectic reaction at T_2 . This should limit the number of nuclei, as well as develop aligned grain growth. At first, samples were heated up to the first sintering temperature (T_1) with a rate of $10^\circ\text{C}/\text{min}$, and held for 0.3h. Then they were cooled to the second sintering temperature (T_2) at a rate of $10^\circ\text{C}/\text{min}$, and held for several hours. Finally the samples were cooled down to 800°C at a rate of $0.5^\circ\text{C}/\text{min}$. The entire sintering procedure was carried out in an oxygen atmosphere.

After sintering, all the samples were annealed at 500°C for 20 hours in an oxygen atmosphere.

Table 1 summarizes the experiments which were conducted using this technique.

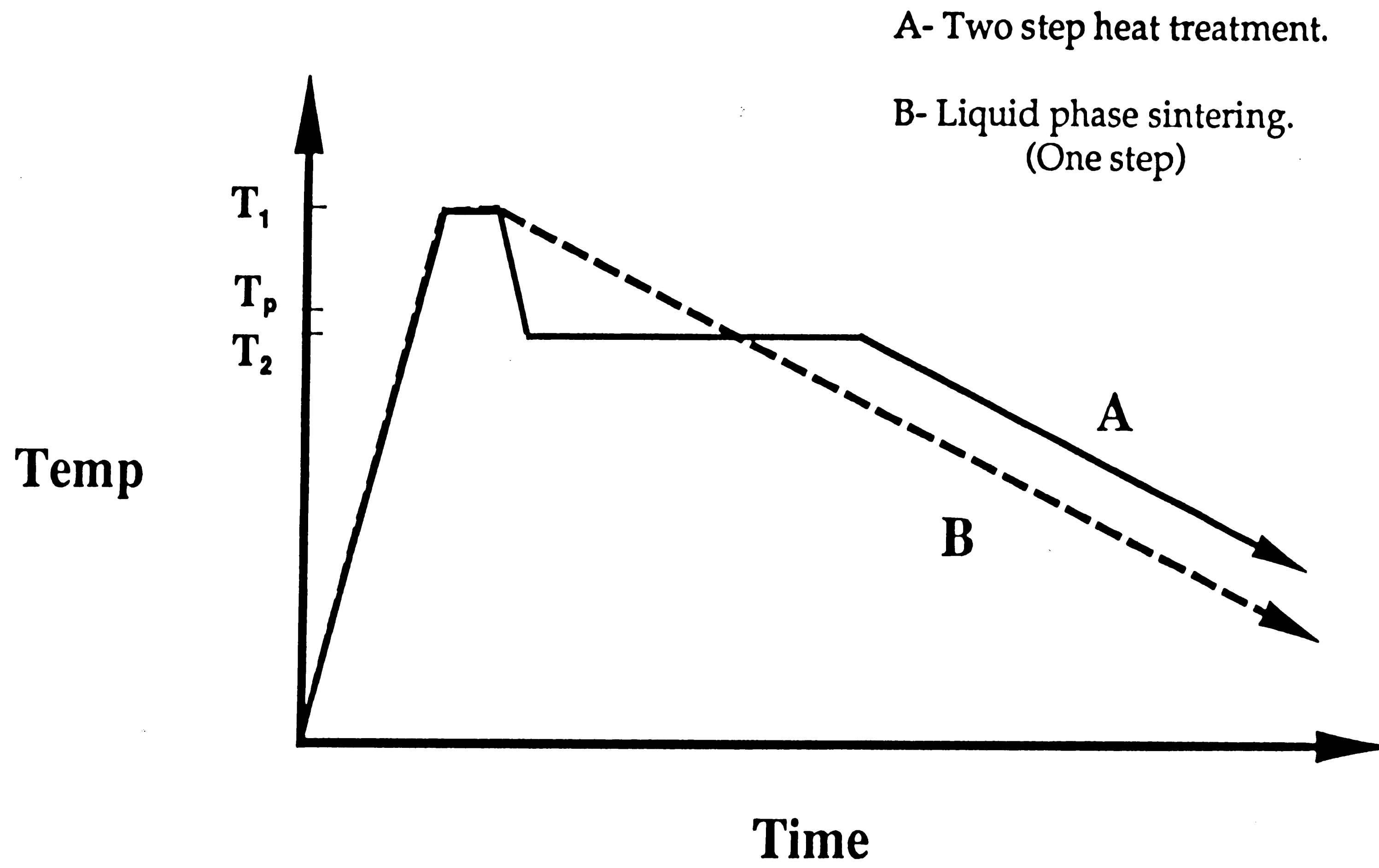


Fig.4 Schematic diagram of two kinds of thermal treatment.

Samples	First Sintering Temperature T₁ (°C)	Hold Time (hr)	Heating rate °C/min (to T₁)	Cooling rate °C/min (to T₂)	Secondary Sintering Temperature T₂ (°C)	Hold Time (hr)	Cooling rate °C/min (to 800 °C)
TST-A	1050	0.3	10	10	950	5.0	0.5
TST-B	1050	0.3	10	10	970	5.0	0.5
TST-C	1050	0.3	10	10	1000	5.0	0.5
TST-D	1050	0.3	10	10	1010	5.0	0.5
TST-E	1010	0.3	10	10	980	5.0	0.5
TST-F	1010	0.3	10	10	970	5.0	0.5
TST-G	1000	0.3	10	10	970	5.0	0.5

TABLE-1. Experimental Data of Thermal Step Treatments

2.4 Seeding-induced Aligned Microstructure

It should be feasible to increase the volume of individual aligned regions through control of the number density of 123 nuclei. The approach for this technique was to use the 200 μm domains of aligned grains obtained from earlier experiments as "seeds" for grain alignment throughout the sample. The seeds were obtained by crushing the specimen with a mortar and pestle, and using selective sieving to extract particles with sizes between 185-200 microns. It was hoped that by this method, the selected particles would consist primarily of individual domains, the reasoning being that fracture would occur preferentially at the domain boundaries. The seeds were added to the conventional 123 powder, such that the bulk samples contained seeds with weight fractions varying from 20wt% to 1wt%. These samples were then sintered. The sintering temperature was varied from 950°C to 1050°C with heating rate 8°C/min, with a hold for 0.5 hours in O₂. Then the samples were cooled down to 800°C at a rate of 0.5°C/min, followed by furnace cooling down to room temperature. The samples were subsequently annealed for 20 hours at 500°C in flowing oxygen .

3 RESULTS AND DISCUSSION

3.1 In-situ Annealing Studies

The in-situ annealing studies revealed that there was localized melting at the grain boundaries, at temperatures $>450^{\circ}\text{C}$. On cooling to room temperature, a discrete second phase was observed at the grain boundaries, as shown in Fig.5. In addition, there also appeared to be some surface reaction, the extent of which varied from grain to grain. For different sintering temperatures, the results showed that the volume fraction of the second phase increased as the maximum temperature increased. Energy-Dispersive X-ray Spectroscopy (EDS) results showed that there was barium in the second phase, but no yttrium or copper. With regard to the second phase composition, X-ray mapping in the electron microprobe showed that it consisted only of the elements carbon, oxygen, and barium, shown in Fig. 6.

Using Wavelength-Dispersive Spectroscopy (WDS), quantitative chemical analysis was performed on both the matrix and the second phase. The results are summarized in Table 2. The matrix analysis showed that the experimental results closely agreed with those of the expected bulk composition ($\text{YBa}_2\text{Cu}_3\text{O}_{6.5}$), thus increasing confidence in the compositional data for the second phase. The second phase along the grain boundaries was identified to be a barium oxycarbonate, with a nominal composition of $\text{BaCO}_{4.8}$.

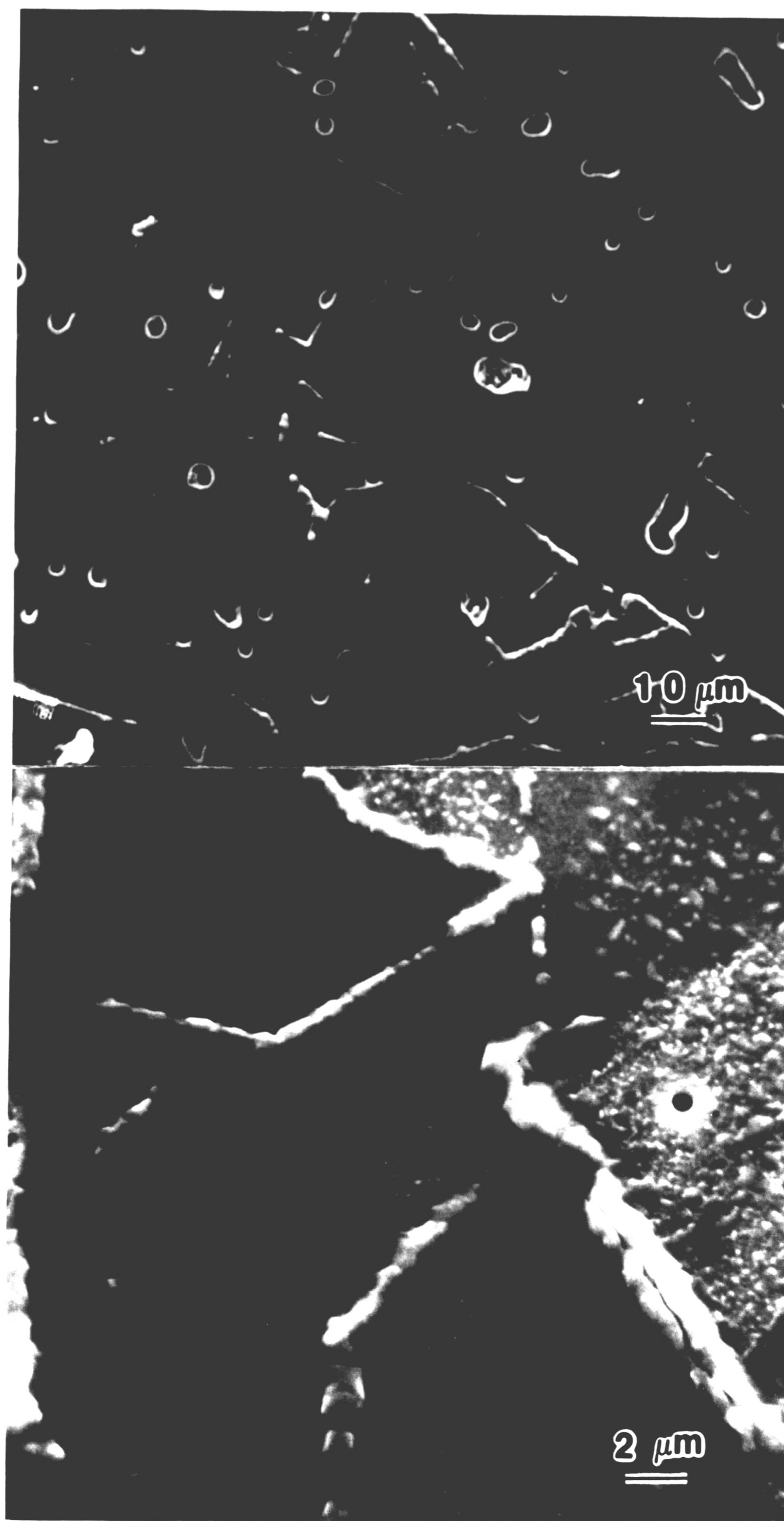


Fig. 5 SEM photographs showing a grain-boundary second phase in a $\text{YBa}_2\text{Cu}_3\text{O}_{6+x}$ sample heated to 700°C in the optical hot-stage.

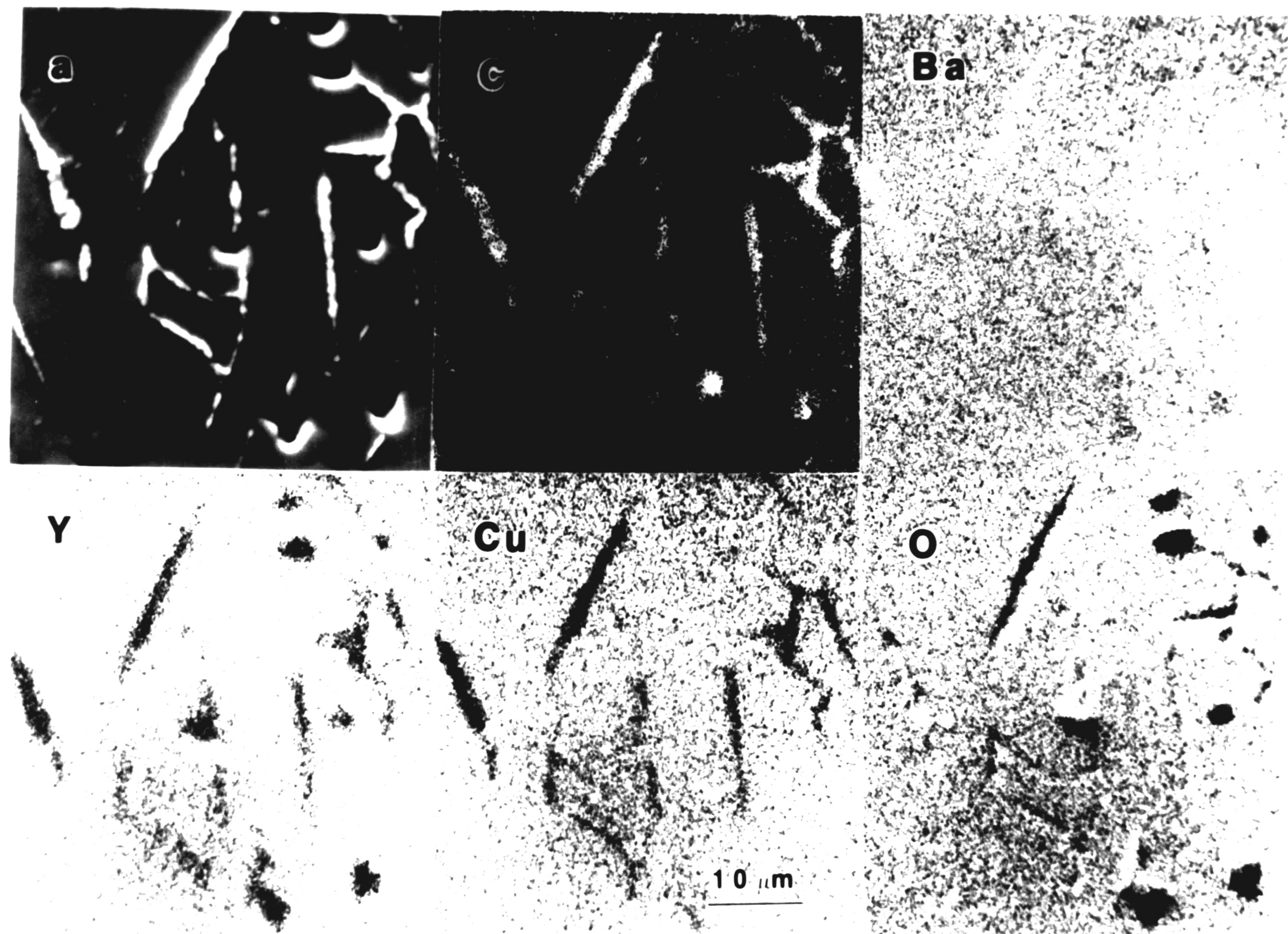


Fig. 6 X-ray maps showing the relative variation in Carbon, Barium, Yttrium, Copper, and oxygen contents between the matrix and the second phase. The conventional secondary electron image is shown in (a).

	Composition (wt%)				
	Y	Ba	Cu	O	C
Matrix: Experimental	14.25±0.28	41.40±0.48	28.50±0.29	15.85±0.64	
Calculated	13.50	41.70	29.00	15.80	
Second phase plus matrix	4.44±0.57	53.63±1.80	8.67±1.28	29.42±1.85	3.84±0.31
Second phase only		58.99±1.98		35.45±2.23	5.56±0.45

Table.2 Results of chemical analysis using X-ray wavelength dispersive spectroscopy.

Transport critical current measurements were performed at 77K at zero magnetic field using a four-probe arrangement, using Gallium as current poles at the ends of the bulk, Indium as electrodes at the middles of the bulk. Fig.7 shows the voltage versus current density for an oxygen-annealed specimen and a specimen annealed for 2 hours at 800°C in air. Both samples were subsequently annealed for 20 hours in flowing oxygen at 500°C. The critical current (J_c) for the air-annealed sample was approximately a factor of 4 less than that of the unannealed sample.

In order to determine the origin of the carbon in the second phase, two likely possibilities were identified: organic polishing cleaning media and atmospheric CO_2 . To avoid contact with water, the $\text{YBa}_2\text{Cu}_3\text{O}_{6+x}$ samples were polished in kerosene, and washed in ethanol. Therefore, carbon contamination of grain boundary regions possibly occurred by seepage of the cleaning media along grain-boundary microcracks induced by mechanical polishing. To test this hypothesis, it was necessary to introduce cracks in the microstructure that were not associated with a grain boundary. This was achieved by making a series of Vickers indentations on two identical polished samples. The indentation load was deliberately chosen to introduce significant radial cracking at the corners of the indentations. One specimen was immersed in ethanol for 12 hours, and the other was used as a control. Both samples were then annealed in air for 2 hours at 800°C. A Scanning Electron Microscope (SEM) photograph shows the region surrounding an indentation for the ethanol immersed sample in Fig.8. There is no preferential formation of the second phase at the radial crack sites. This result is persuasive evidence that the formation of the carbon-contamination second phase is unrelated to contamination by the organic polishing cleaning media. Therefore, the carbon in the second phase most likely comes from air.

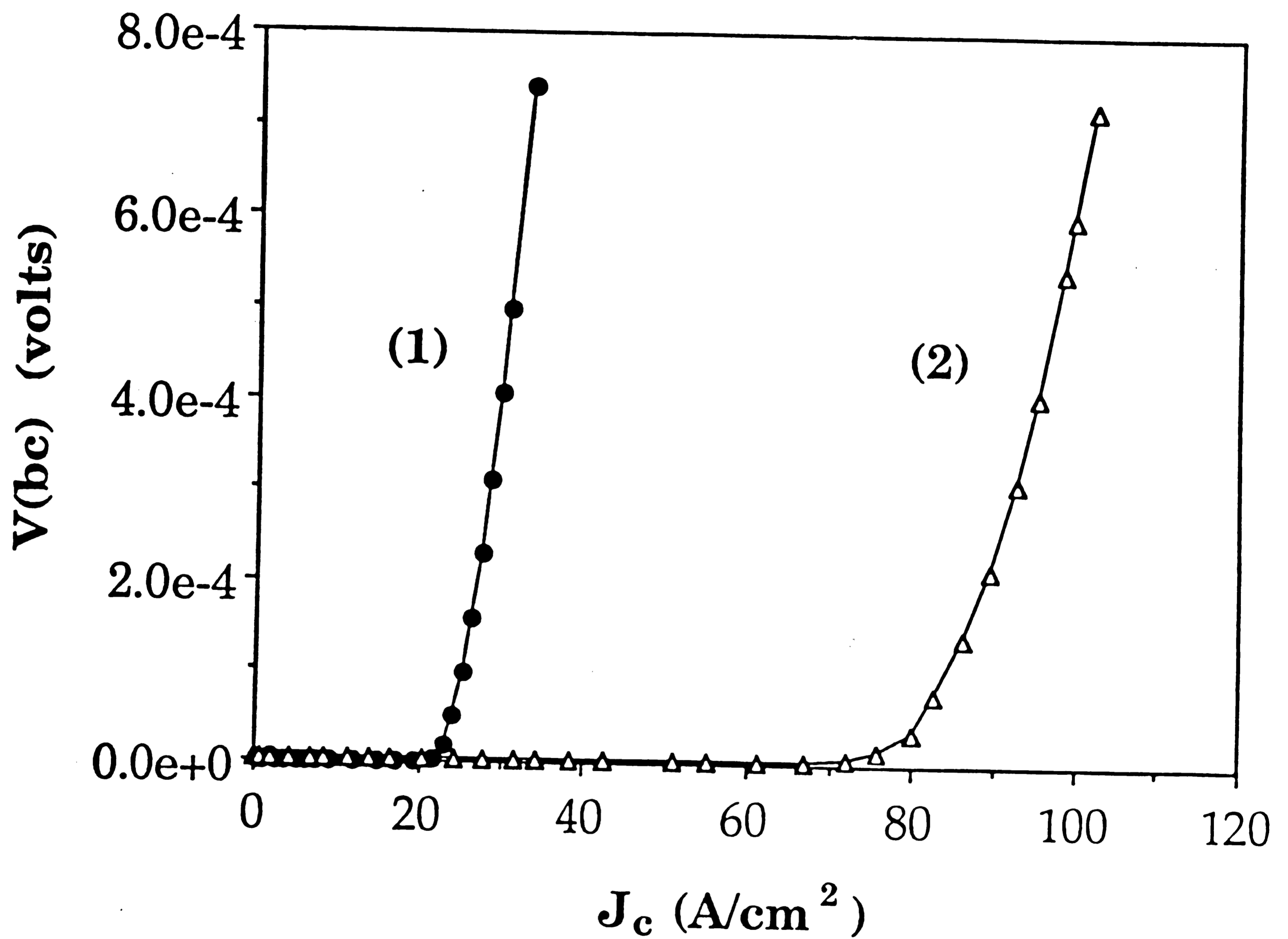


Fig. 7 Comparison of voltage versus current density curves for $YBa_2Cu_3O_{6+x}$ specimens: (1) air annealed for 2 hr at $800^\circ C$ and (2) oxygen annealed for 10 hr at $800^\circ C$. Both samples were subsequently annealed in flowing oxygen at $500^\circ C$ for 20 hr (77K, zero magnetic field).

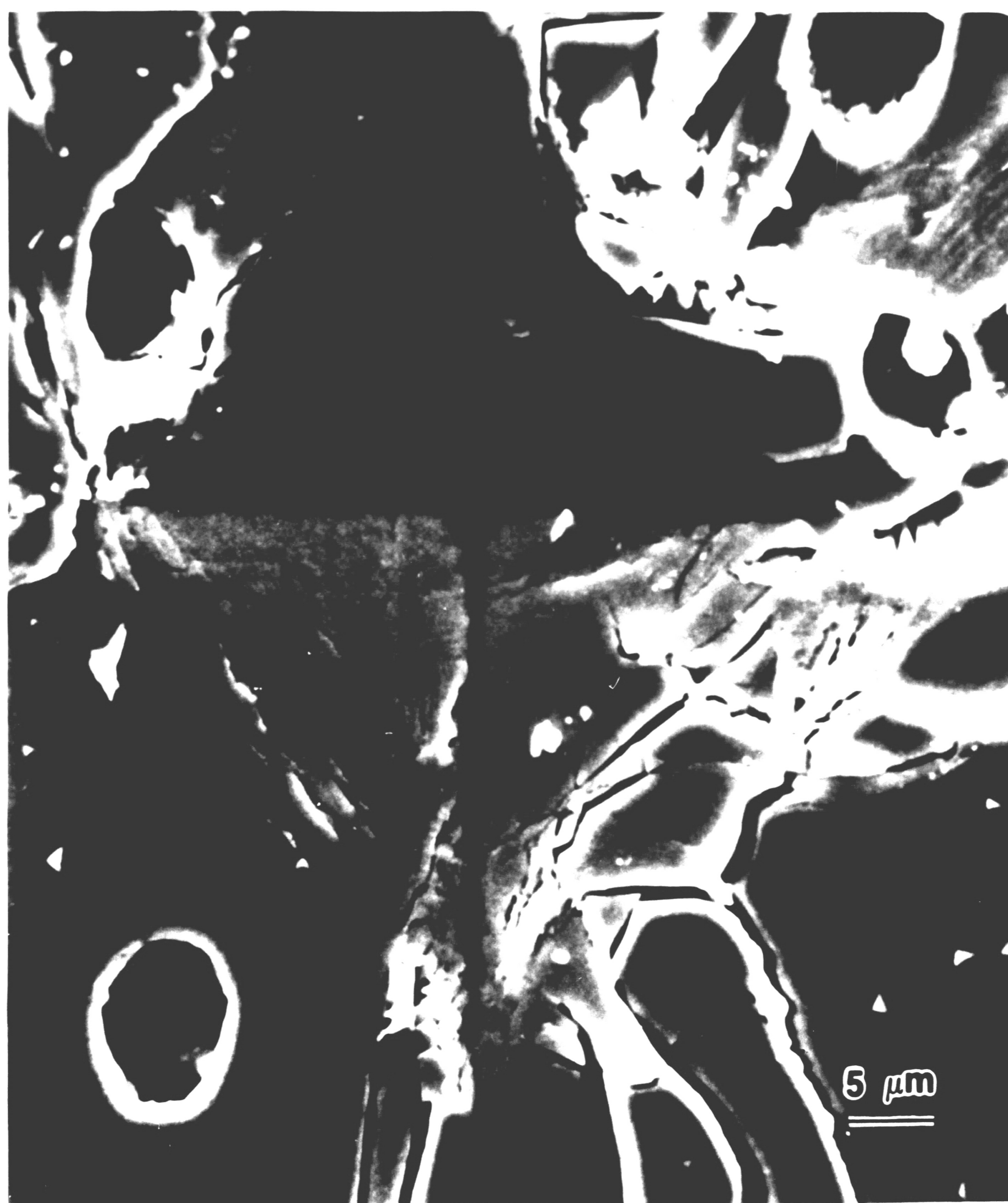


Fig. 8 SEM photograph showing an indentation site in a $\text{YBa}_2\text{Cu}_3\text{O}_{6+x}$ specimen immersed 12 hr in ethanol and annealed 2 hr at 800°C in air.

Since initial annealing of the $\text{YBa}_2\text{Cu}_3\text{O}_{6+x}$ specimens was performed in air, a possible source of the carbon was atmospheric carbon dioxide. To test the effect of different annealing atmospheres, one polished specimen of $\text{YBa}_2\text{Cu}_3\text{O}_{6+x}$ was annealed in 99.9% pure oxygen for 2 hours at 800°C , and the other was given the same heat treatment, but was annealed in pure CO_2 . SEM examination of surfaces showed that, for the sample annealed in oxygen, no grain-boundary second phase was observed. For the CO_2 -annealed sample, the entire specimen surface was covered with second phase, as shown in Fig.9. Qualitative analysis showed that the second phase consisted of barium, oxygen, and carbon only. To check the reversibility of the second-phase formation, the CO_2 -annealed sample was reannealed in pure oxygen for 2 hours at 800°C . There was no change in the volume fraction of the second phase. These results confirmed the hypothesis that the second phase formed as a result of contamination from atmospheric CO_2 .



Fig. 9 SEM photograph showing a $\text{YBa}_2\text{Cu}_3\text{O}_{6+x}$ sample surface covered with Ba-C-O second phase. Sample annealed 2 hr at 800°C in CO_2 .

3.2 Influence of Thermal Processing on Texture Formation

3.2.1 One-step Thermal Treatment

The microstructure, specifically the phases present, is very sensitive to small variations in processing conditions. This sensitivity to small changes in temperature, hold time or cooling rate, may dominate the properties of $\text{YBa}_2\text{Cu}_3\text{O}_{6+x}$.

1). Effect of Sintering Temperature

No significant grain alignment was obtained for sintering temperatures below 970°C or above 1070°C . Note that in the above series of experiments, the cooling rate was kept constant at $0.5^\circ\text{C}/\text{min}$, and the hold time was 2 hours.

The optimum sintering temperature was found to be 1050°C , because the samples sintered at this temperature showed a high degree of alignment, and relatively little second phase. For this reason, subsequent experiments were performed using a sintering temperature of 1050°C .

2). Effect of Sintering Hold Time

The sintering hold time (T_h) was varied from 0.5 hour to 20 hours at the sintering temperature 1050°C , with a cooling rate of $0.5^\circ\text{C}/\text{min}$ down to 800°C . The results showed that for hold times longer than 8 hours, the degree of alignment was less. The microstructures of the sintered samples showed that short sintering time results in less second phase. The size of the aligned regions decreased as holding time was increased.

3). Effect of Cooling Rate

A series of specimens was prepared in which the cooling rate was varied from 0.1°C/min to 4°C/min at the sintering temperature 1050°C, with a hold of 2 hours. The results showed that for a cooling rate of 4°C/min, less alignment was obtained. For cooling rates of 0.1°C/min and 0.5°C/min, the same high degree of alignment was obtained. Therefore, the cooling rate of 0.5°C/min was chosen for convenience.

From the results of the above experiments, the optimum (one-step) heat treatment in terms of inducing grain alignment was found to be 0.5 hour at 1050°C at a cooling rate of 0.5°C/min. The microstructure of a specimen subjected to such a heat treatment is shown in Figure 10. The microstructure of the specimen consisted of aligned regions (called domains) approximately 200 microns in size. Within each individual domain, the grains were highly elongated and showed very good alignment. The orientation difference between adjoining domains was random. EDS results showed that there were three kinds of second phase found in the samples. 1) Cu or CuO-rich, 2) Ba-rich second phase, and 3) a Y-rich second phase (Y_2BaCuO_5). Also there were some pores and cracks between the aligned regions. The second phases which formed from decomposition of $YBa_2Cu_3O_{6+x}$ at high temperature are unstable at room temperature. Further, they have strong chemical activity with water which completely destroyed the electronic properties and microstructure of the specimen. They became green and brown in color rather than black. The heating rate did not influence the texture.

For development of a textured microstructure, a sufficient amount of liquid phase is necessary during sintering. $YBa_2Cu_3O_{6+x}$ powder decomposes to 211 phase and liquid phase above the peritectic temperature. An appropriate amount of liquid phase and a certain 211 grain size affect the texture by promoting highly anisotropic grain growth.

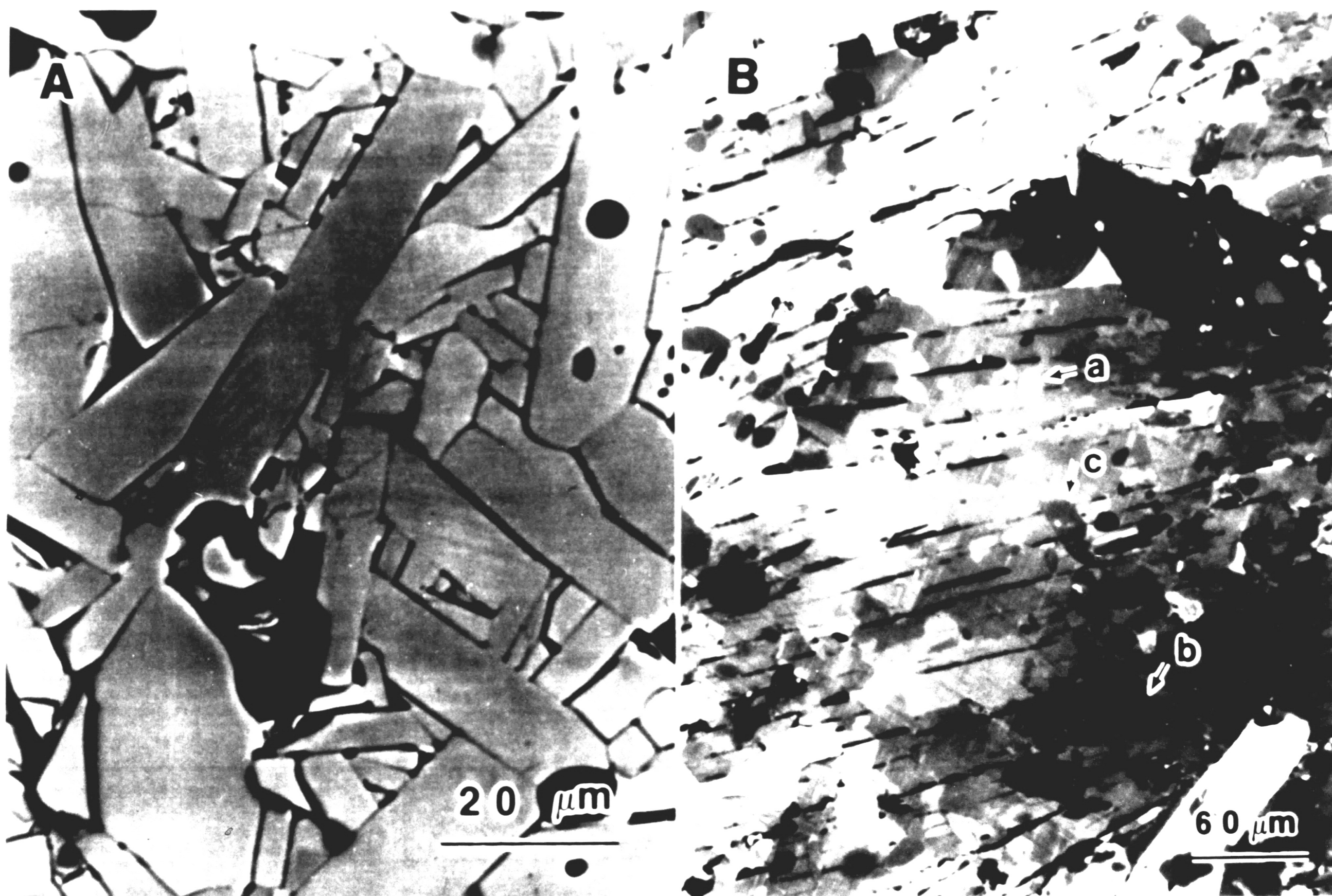
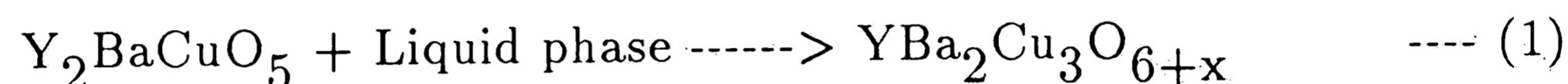


Fig. 10 SEM micrographs showing (A) conventional sintered $\text{YBa}_2\text{Cu}_3\text{O}_{6+x}$ microstructure, sintered 20 hours at 920°C ; (B) aligned regions in $\text{YBa}_2\text{Cu}_3\text{O}_{6+x}$ sample sintered 0.5 hours at 1050°C , in O_2 ; second phases indicated by arrows a: 211 phase, b: Cu-rich phase, and c: Ba-rich phase.

3.2.2 Quench experiments

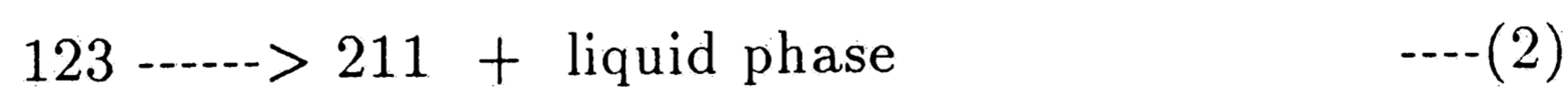
When $\text{YBa}_2\text{Cu}_3\text{O}_{6+x}$ is heated up above the peritectic temperature (1002°C) in an oxygen atmosphere, it decomposes into Y_2BaCuO_5 (the "green" phase or "211") and a liquid phase [56, 57]. During cooling, the reverse reaction occurs at approximately 1002°C :



For reference, the corresponding section of the $\text{BaO} \cdot \text{Y}_2\text{O}_3 \cdot \text{CuO}$ phase diagram is shown in Fig. 11 [58].

To determine the mechanism by which highly aligned structures develop in 123, a series of specimens was quenched at different temperatures during the heating and cooling stage from 950°C to 1050°C . It was hoped that the results of these quenching experiments would identify the point at which the texture begins to develop.

For specimens quenched during the heating stage, SEM observations showed that the volume fraction of second phases increased as the quench temperature increased from 950°C to 1050°C . However, no evidence of grain alignment was observed (Fig 12). As the quenching temperature (i.e. sintering temperature) was increased, the amount of second phases of 211 and liquid were obviously increased as the reaction proceeded:



Unfortunately examination of the microstructure of the quenched specimens was made difficult by the fact that they reacted severely with the polishing lubricants, such as

water, kerosene and pure ethyl alcohol.

During the cooling stage, the volume fraction of the second phases decreased as the quench temperature decreased from 1050°C to 1010°C. Again there was no alignment in the specimens. However, aligned regions appeared in the specimens which were quenched from below 1000°C during the cooling stage, see in Fig.13.

Quench tests revealed that the $\text{YBa}_2\text{Cu}_3\text{O}_{6+x}$ decomposed into Y_2BaCuO_5 ("211") and a liquid phase as the heating temperature increased above 1000°C. The cooling rate was found to be important to the texture formation. It is postulated that the effect of slow cooling is to minimize gradients in oxygen content, so that transformation strains tend to develop uniformly throughout a grain. During slow cooling, the peritectic reaction reversed occurred following the equation (1), forming the 123 phase, and causing grain growth. Also, slow cooling allows sufficient time for oxygen diffusion. Careful control of the processing can lead to the formation of optimized samples. For improving the texture, the sintering temperatures, hold time, and the cooling rate, are very critical parameters. The critical sintering temperature was around 1000°C, with an optimal cooling rate below 1°C/min.

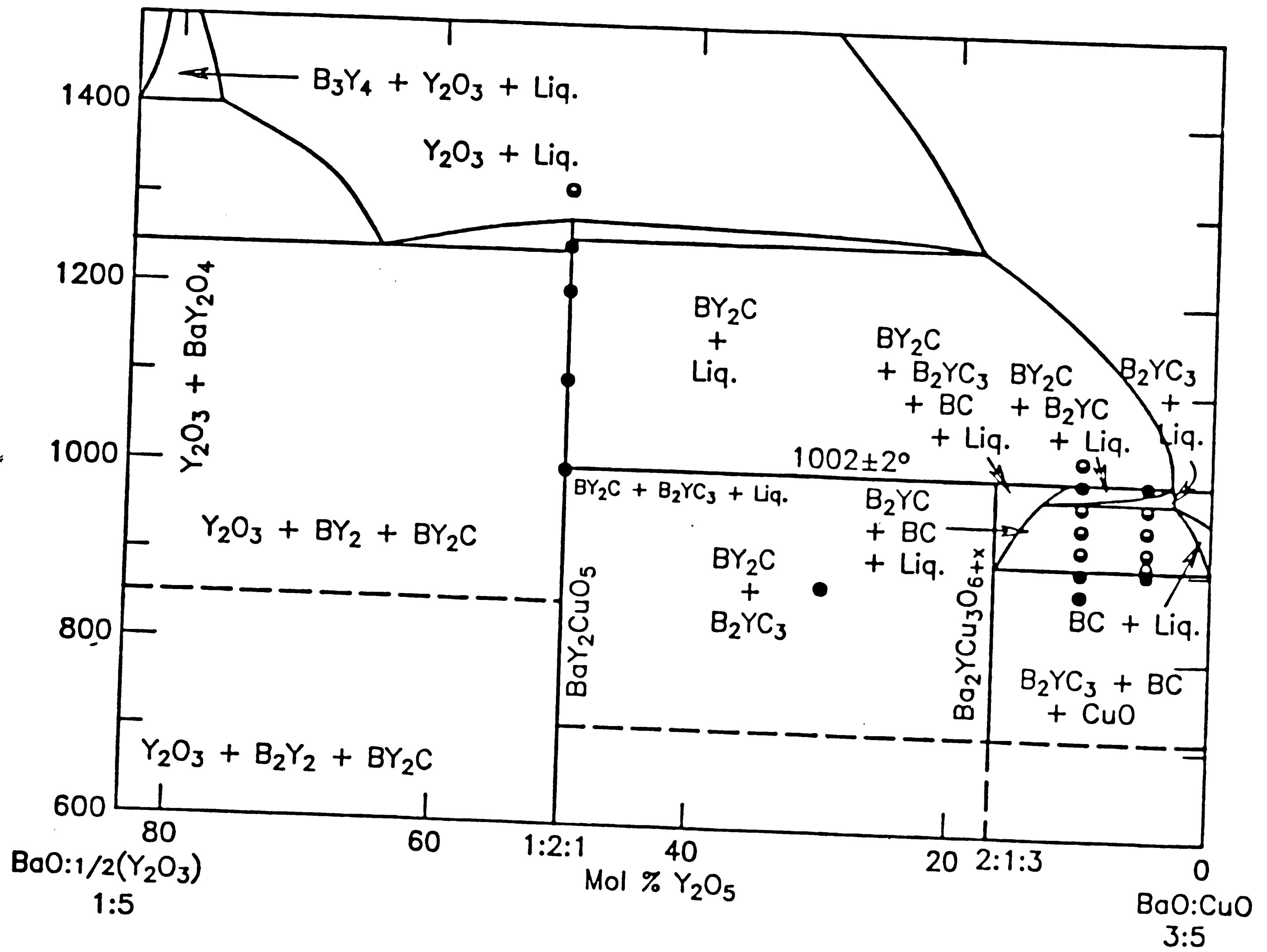


Fig.11 Section through $\text{BaO} \cdot \text{Y}_2\text{O}_3 \cdot \text{CuO}$ phase diagram.

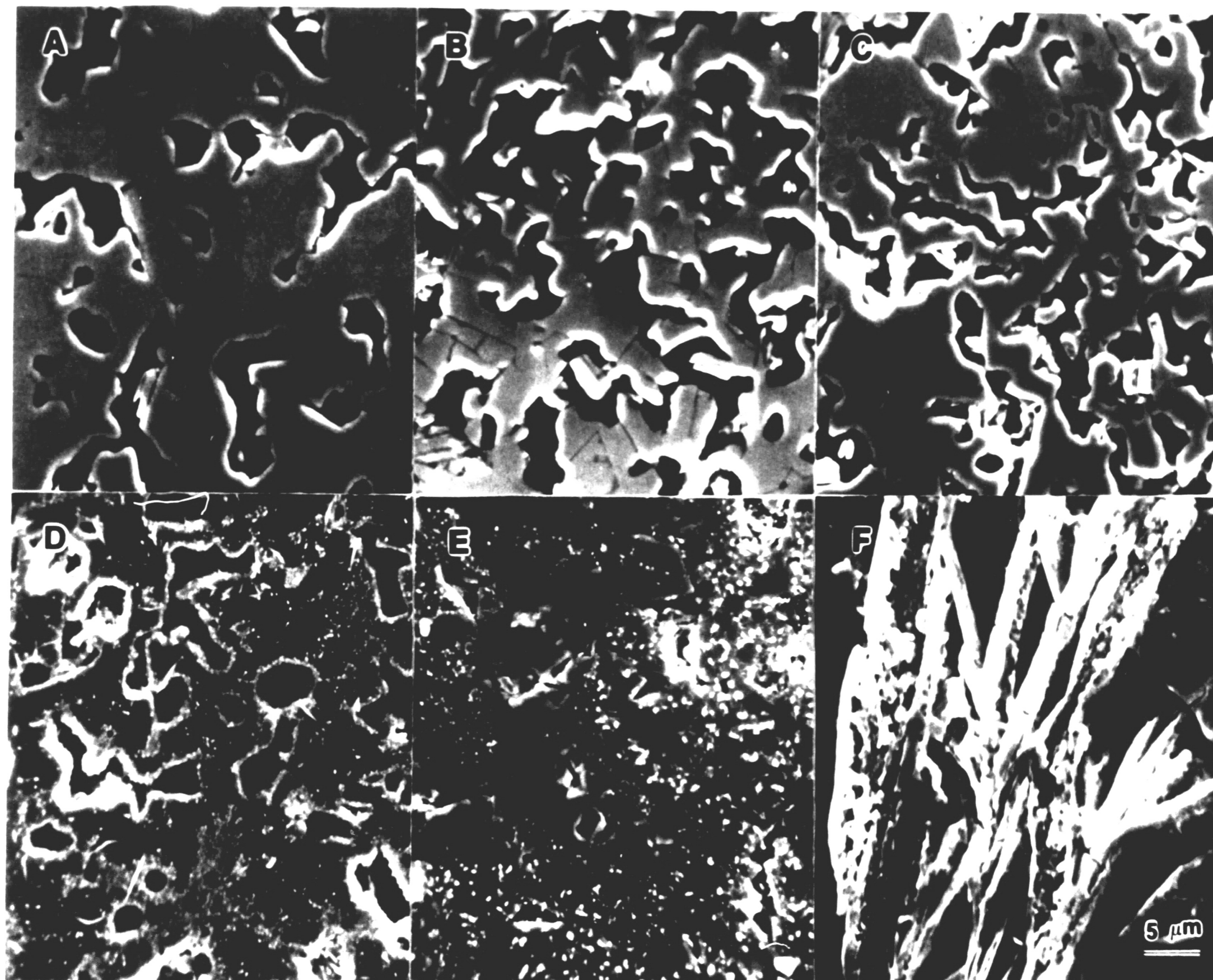


Fig. 12 SEM micrographs of samples quenched during heating stage. Quench temperature A: 950°C , B: 970°C , C: 990°C , D: 1010°C , E: 1030°C , F: 1050°C . Note absence of grain alignment.

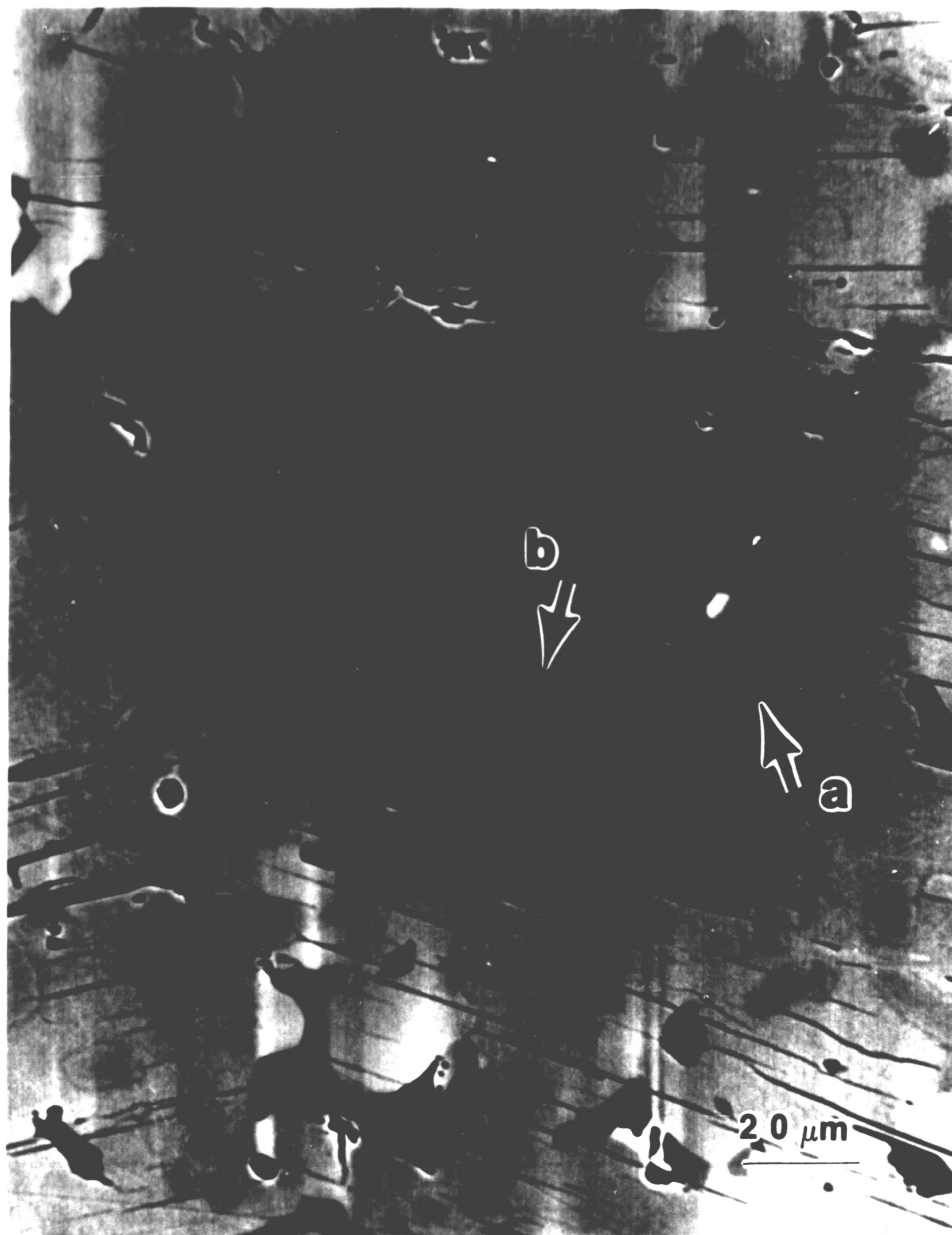
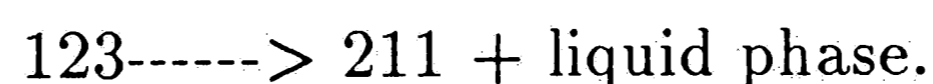


Fig. 13 SEM micrograph of sample quenching from 900°C during the cooling stage
second phases depicted by arrows a: 211 phase, b: CuO.

3.2.3 Two-Step Thermal Treatment

The results from the two-step thermal treatment experiments showed a dramatic improvement in the degree of alignment over the samples heat-treated at a single temperature. Of the heat-treatment sequences tried (see Table 1), the optimum one was found to be heating at temperature 1050°C (T_1) and holding 0.3 hours (which is necessary to provide a sufficient amount of liquid phase), followed by cooling rapidly ($10^{\circ}\text{C}/\text{min}$) down to 970°C (T_2), and holding 5 hours. Finally, samples were slowly cooled down to 800°C ($0.5^{\circ}\text{C}/\text{min}$). This produced a domain size of 2mm, as seen in Fig. 14. The samples consisted mostly of the $\text{YBa}_2\text{Cu}_3\text{O}_{6+x}$ superconducting phase. There were other phases located between domains, but the volume of the second phases was greatly reduced compared to the other sintered samples (TST-C, TST-D, see Table 1).

The reason for the improved alignment with the two-step heat treatment is believed to be as follows. The first stage of the heat-treatment, annealing above the peritectic temperature (T_p) allows partial transformation of the 123 according to the reaction



The hold time determines the extent to which this reaction goes to completion. On cooling below T_p , it is thought that the unreacted 123 act as heterogeneous nuclei for the reverse reaction

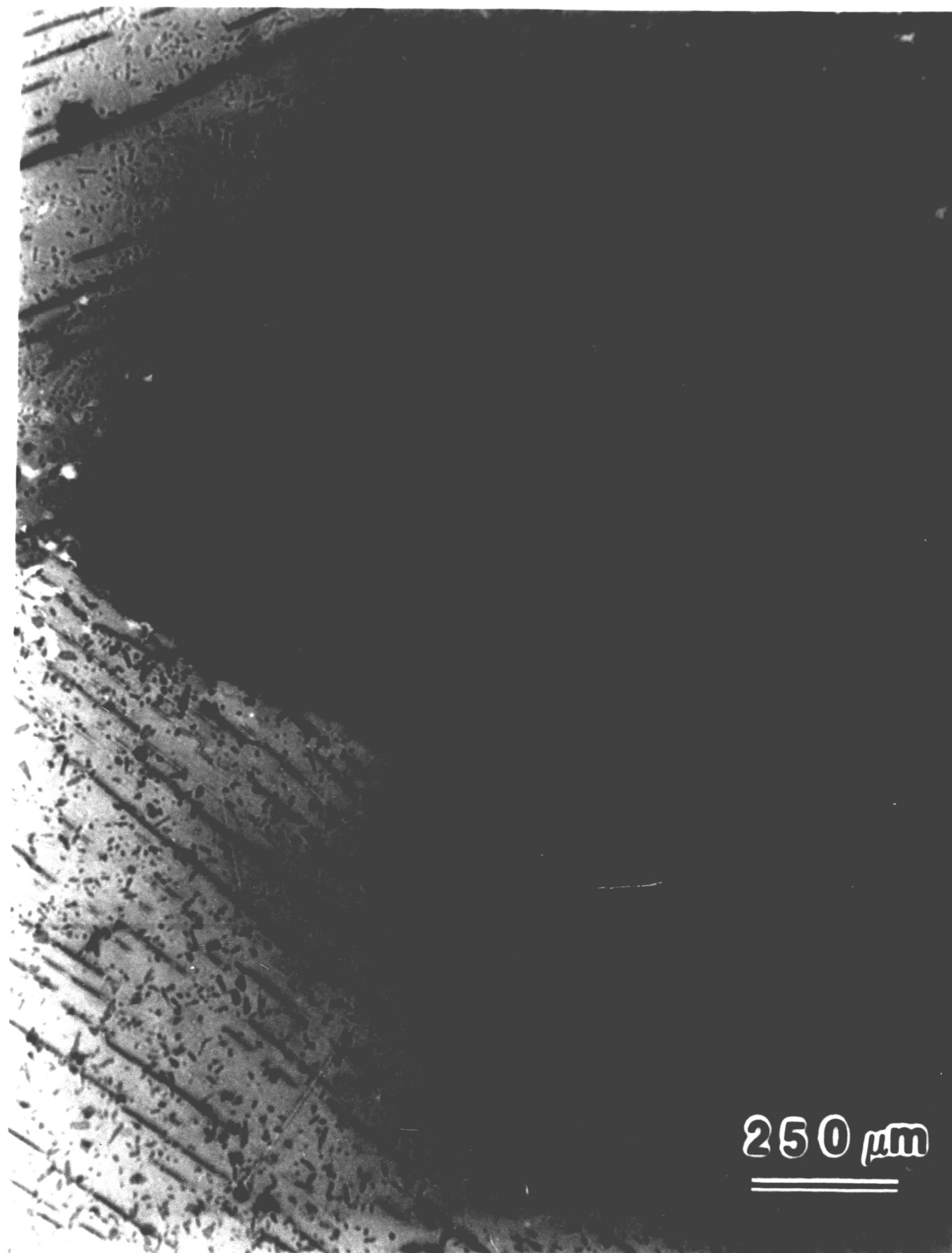


Fig. 14 Optical micrograph of 123 sample after thermal step treatment (1050°C/970°C, second stage hold time $H_2=5$ hrs, in O_2). Domain is > 2 mm in size.

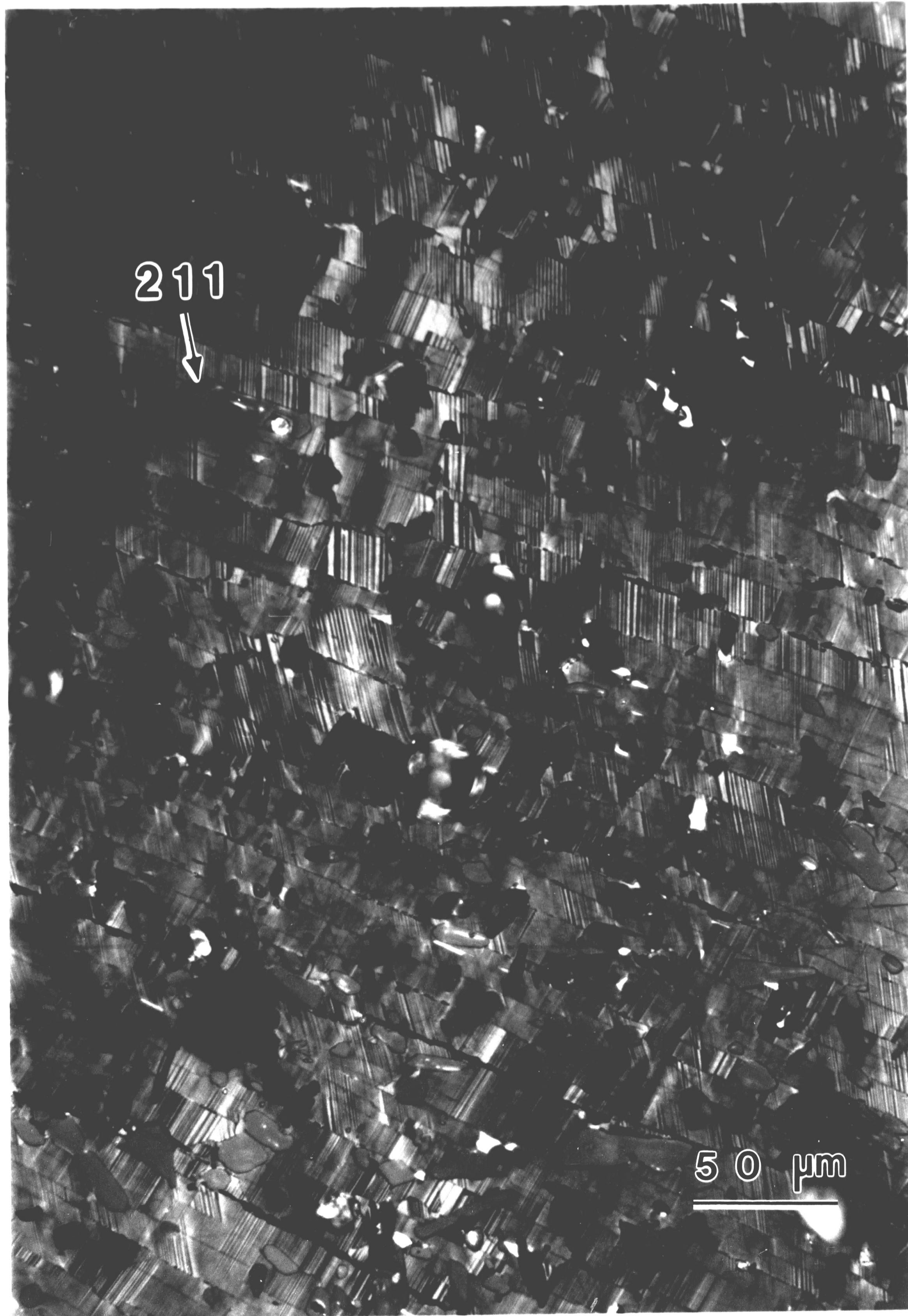


Fig. 15 Optical micrograph of two-step heat treatment sample ($1050^{\circ}\text{C}/970^{\circ}\text{C}$, $\text{H}_2=5$ hrs, in O_2) by polaroid. Twinning within the grains is clearly evident. The second phase particles are 211.

211 + liquid phase -----> 123 (aligned)

It is thought that the grain alignment arises from a combination of growth rate anisotropy and surface energy anisotropy [59]. During melt processing, the grain growth anisotropy arises from the anisotropy in the mass transport rate between the a-b and c planes. The a and b axes are rapid growth directions and form a diffuse interface. This has been described by Hepp et al [59] who observed 123 platelets with stepped growth ledges parallel to the c-axis.

Jin et al [39] predicted that grain growth during melt processing was likely to result in impurities and second phases being 'swept' ahead of the growth front. The thermal step treatment results supported this, where the second phases were pushed away to the side between the aligned regions, as shown in Fig. 16. This effect may be beneficial, since the segregated second phases are less likely to interfere with supercurrent flow within the domains.

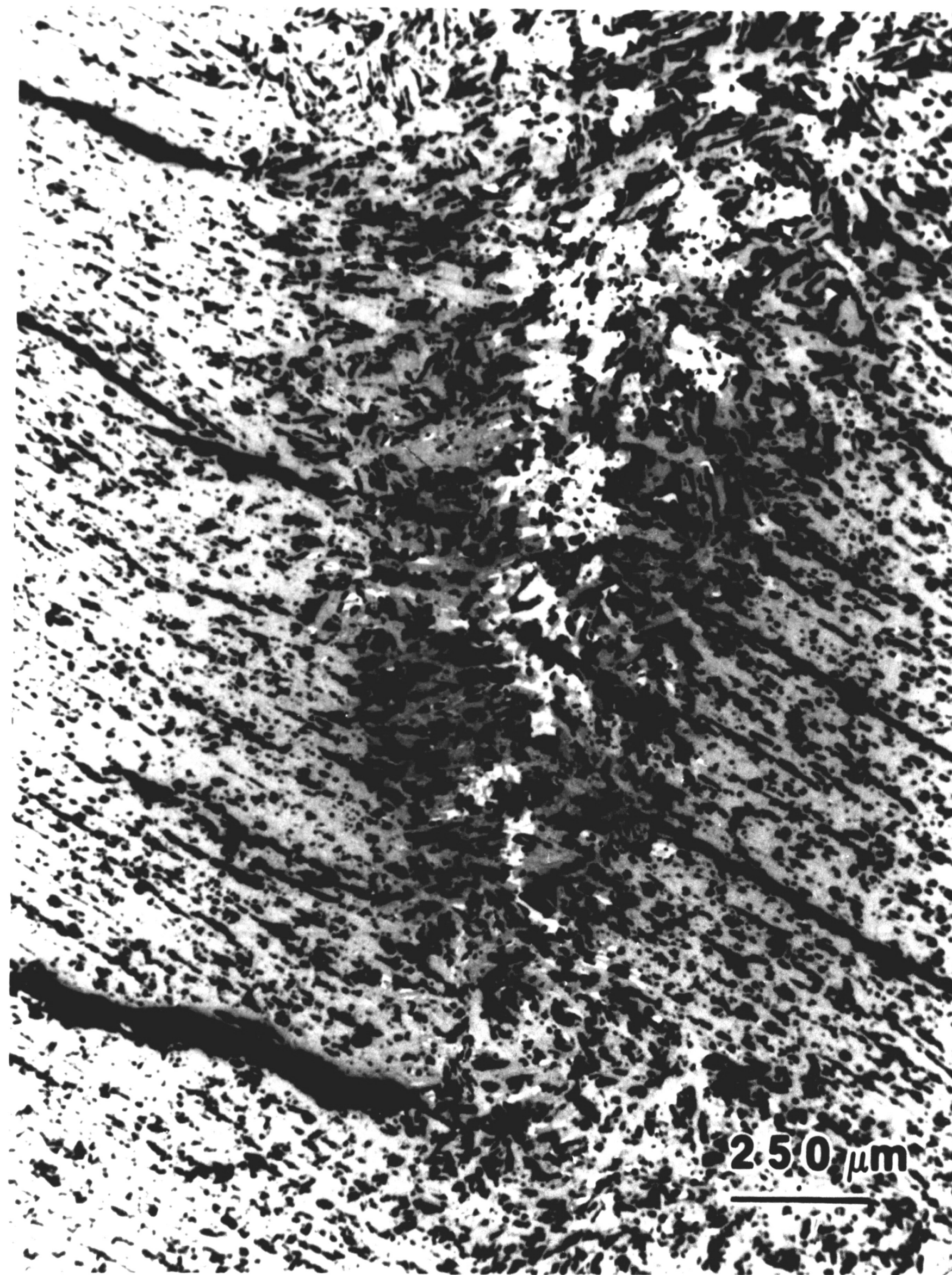


Fig. 16 Optical micrograph of $\text{YBa}_2\text{Cu}_3\text{O}_{6+x}$ sample after thermal step treatment ($1050^\circ\text{C}/970^\circ\text{C}$, $\text{H}_2 = 5$ hrs, in O_2) showing impurities between domains.

3.3 Texture by Seeding

Preliminary experiments showed that the optimum condition involved adding \leq 3wt% seeds (200 micron), and then sintering at 1010°C. Using this method, the domain size was larger than that obtained by one-step melt processing at 1050°C. The domains in the seeded samples were about 1mm in size, as shown in Fig. 17. In a given domain, the grain alignment is very pronounced. The sample as a whole contains few pores and has a higher density compared to the density of a conventional sintered sample. Microcracks, due to thermal expansion anisotropy, occur along grain boundaries. Most of the second phase particles within the domains are 211. Increasing the content of seeds above 5wt % did not improve the size of the aligned regions.

Compared to conventionally processed 123 samples, the critical current density of the seeded sample was increased by an order of magnitude (Fig.18). This improvement is believed due to the alignment and orientation of grains in the superconducting $\text{YBa}_2\text{Cu}_3\text{O}_{6+x}$, which help eliminate the weak link between grains at high angle grain boundaries.

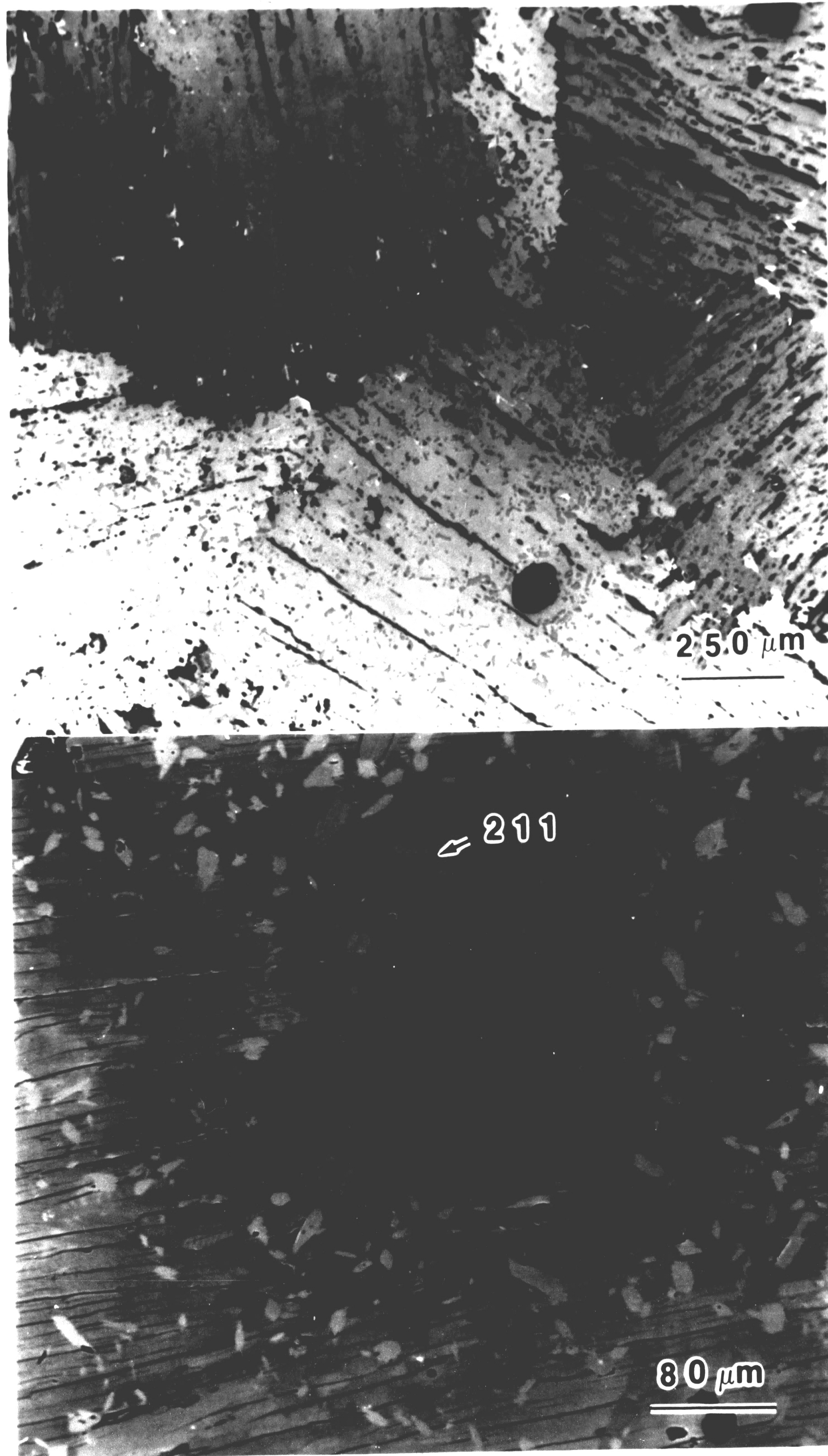


Fig. 17 Optical micrograph of seeded 123 specimen showing a, regions (1mm) of highly aligned grains, b, within aligned domain, second phase particles of 211.

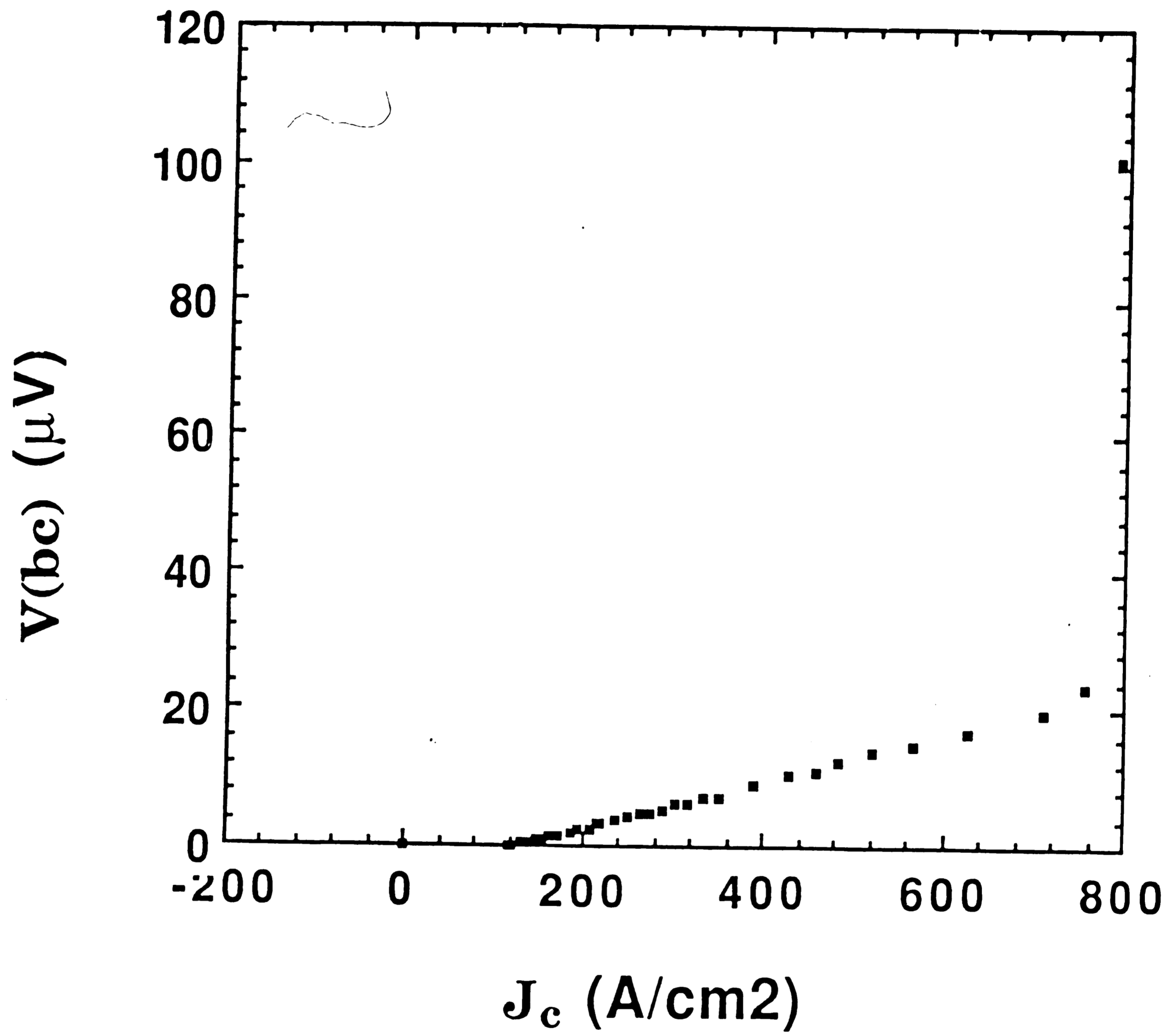


Fig. 18 Current density for seeded 123 specimens, sintered at 1010°C, 1/2 hour, in O₂.

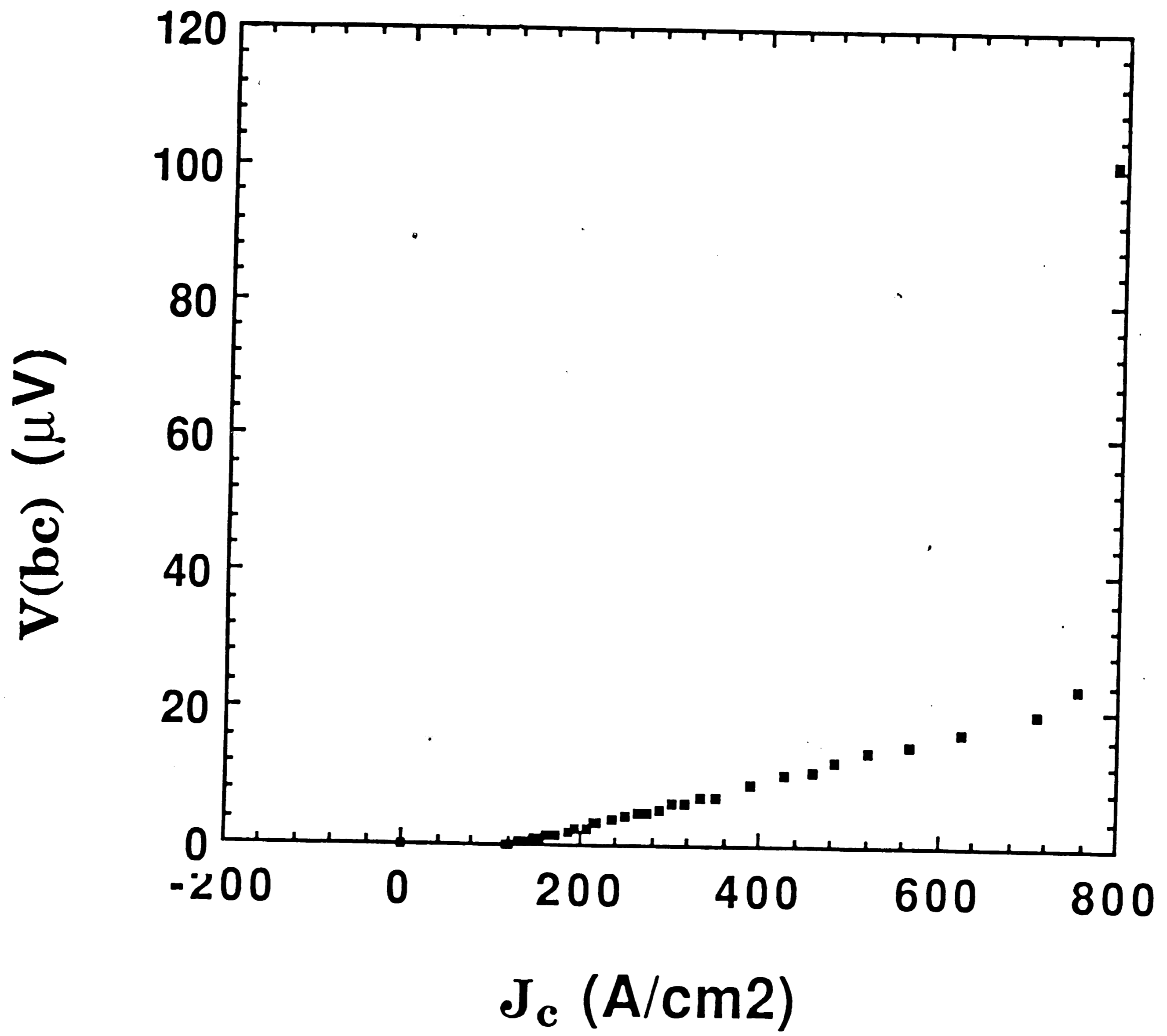


Fig. 18 Current density for seeded 123 specimens, sintered at 1010°C, 1/2 hour, in O₂.

4 SUMMARY AND CONCLUSIONS

1. A carbon-containing second phase $\text{BaCO}_{4.8}$ is formed at grain boundaries during heat treatment at temperatures above 450°C in air. This results from a reaction between $\text{YBa}_2\text{Cu}_3\text{O}_{6+x}$ and carbon dioxide in the atmosphere, which appears to be irreversible.

2. i). Melt processing (i.e. annealing at temperatures greater than the peritectic temperature) produces regions of aligned grains of 200 microns in size. The optimum heat treatment was found to be heating at 1050°C , holding 0.5 hours, and cooling at a rate of $0.5^{\circ}\text{C}/\text{min}$ down to 800°C in oxygen atmosphere. The cooling rate near the peritectic temperature strongly affects the degree of texture. A slow cooling rate, such as $0.5^{\circ}\text{C}/\text{min}$, favors a textured microstructure. The heating rate, however, did not influence the texture. The enhanced alignment (relative to conventionally sintered samples) is believed to be due to growth and surface energy anisotropy of $\text{YBa}_2\text{Cu}_3\text{O}_{6+x}$ in the presence of the liquid phase.

ii). A two-step heat treatment greatly improved the degree of texture, increasing the domain size to 2mm. It is thought that the heat-treatment at the two annealing temperatures (one above T_p , and the other below T_p), correspond to nucleation and growth of the aligned domains.

iii). Textured domains approximately 1mm in size were obtained by incorporating 3wt % "seeds" into the powders. The aforementioned "seeds" consisted of individual domains obtained by crushing and sieving melt-textured specimens obtained by method i).

References:

- [1]. D.R. Clarke, "The Development of High- T_c Ceramic Superconductors: an Introduction", *Adv. Ceram. Mat.*, 2, 3B, (1987), pp. 273-287.
- [2]. M. D. Lemonick, "Superconductors", *Time*, N.Y., May 11, (1987).
- [3]. J. G. Bednorz and K. A. Muller, "Possible High T_c Superconductivity in the Ba-La-Cu-O System", *Zeitschrift Fur Physik*, B64, (1986), pp. 189-193.
- [4]. D. Dimos, P. Chaudhari, J. Mannhart, and F. K. LeGoues, "Orientation Dependence of Grain-Boundary Critical Currents in $YBa_2Cu_3O_{6+x}$ Bicrystals", *Phy. Rev. Lett.* Vol.61, No.2, (1988), pp. 219-222.
- [5]. K. G. Frase, E. G. Liniger and D. R. Clarke, "Environmental and Solvent Effects on Yttrium Barium Cuprate ($YBa_2Cu_3O_x$)". *Ad. Ceram. Mat.*, 2, 3B, (1987), pp. 689-700.
- [6]. X. Jiang, H. Yu, Z. Zhang, N. Zhu, H. Qi, G. Shu, Y. Tian, D. Pang, X. Zeng, and Z. Yang, "Effect of Crystal Structure on Superconductivity of Y-Ba-Cu-O System Compounds", *Appl., Phys., Lett.*, 51(8), (1987), pp. 625-627.
- [7]. C. K. Chiang, L. P. Cook, S. S. Chang, J. E. Blendell and R. S. Roth, "Low Temperature Thermal Processing of $Ba_2YCu_3O_{7-x}$ Superconducting Ceramics", *Ad. Ceram. Mat.*, Vol. 2, No. 3B, (1987), pp. 530-538.
- [8]. J. D. Verhoeven, A. J. Bevolo, R. W. McCallum, E. D. Gibson, and M. A. Noack, "Auger Study of Grain Boundaries in Large-Grained $YBa_2Cu_3O_x$ ", *Appl., Phys., Lett.*, Vol. 52, No., 9, (1988), pp. 745-747.
- [9]. K. C. Goretta, A. J. Schultz, D. W. Capone II, T. L. Tolt, U. Balachandran, J. T. Dusek, M. T. Lanagan, R. B. Poeppel, J. P. Singh, D. Shi, R. L. McDaniel, D. S. Applegate, J. K. Degener, and J. S. Kallend, "Texturing of $RBa_2Cu_3O_x$ Superconductors", *Ceram. supercon.* 2, Research Update, (1988), pp. 323-331.
- [10]. J. P. Singh, U. Balachandran, D. Shi, J. K. Degener and R. B. Poeppel, "Observations of Preferred Orientation in High- T_c Oxide Superconductor Tapes", *Mat. Lett.* Vol. 7, No. 3, (1988), pp. 72-84.
- [11]. M. K. Malik, V. D. Nair, A. R. Biswas, and R. V. Raghavan, "Texture Formation and Enhanced Critical Currents in $YBa_2Cu_3O_7$ ", *Appl. Phys. Lett.*, 52 (18), May, (1988), pp. 1525-1527.
- [12]. C. W. Chu, P. H. Hor, R. L. Meng, L. Gao, Z. J. Huang, and Y. Q. Wang, "Evidence for Superconductivity above 40K in the La-Ba-Cu-O Compound System", *Phy. Rev. Lett.* Vol. 58, No. 4, 1987, pp. 405-407.
- [13]. J. M. Tarascon, L. H. Greene, W. R. McKinnon, and G. W. Hull, "Superconductivity At 90K in a Multi-Phase Oxide of Y-Ba-Cu", *Phy. Rev. B*, 35,

(1987), pp. 7115.

[14]. S. Jin, R. C. Sherwood, T. H. Tiefel, G. W. Kammlott, R. A. Fastnacht, M. E. Davis, and S. M. Zahurk, "Superconductivity in Bi-Sr-Ca-Cu-O Compounds With Noble Metal Additions", *Appl. Phys. Lett.* 52, (19), May (1988).

[15]. Z. Z. Sheng and A. M. Hermann, "Bulk Superconductivity at 120K in the Tl-Ca/Ba-Cu-O System", *Nature* Vol. 332, March, (1988), pp. 138-139.

[16]. R. Beyers, and T. M. Shaw, "The Structure of $\text{YBa}_2\text{Cu}_3\text{O}_{7-x}$ and its Derivatives", *Solid State Physics*, Vol. 42, (1989), pp. 136-145.

[17]. R. J. Cava, B. Battlogg, R. B. van Dover, D. W. Murphy, S. Sunshine, T. Siegrist, J. P. Remeika, E. A. Rietman, S. Zahurak, and G. P. Espinosa, "Bulk Superconductivity at 91K in Single Phase Oxygen-Deficient Perovskite $\text{Ba}_2\text{YCu}_3\text{O}_{9-x}$ ", *Phy. Rev. Lett.* Vol. 58, No. 16, (1987), pp. 1676-1679.

[18]. P. K. Gallagher, "Characterization of $\text{Ba}_2\text{YCu}_3\text{O}_x$ as a Function of Oxygen Partial Pressure; Part1: Thermoanalytical Measurements", *Adv. Ceram. Mat.* 2, 3B, (1987), pp. 632-639.

[19]. H. M. OBryan and P. K. Gallagher, "Characterization of $\text{Ba}_2\text{YCu}_3\text{O}_x$ as a Function of Oxygen Partial Pressure; Part 2: Dependence of the Orthorhombic-Tetragonal Transition on Oxygen Content", *Ad. Cera. Mat.* 2, 3B, (1987), pp. 604-648.

[20]. Donglu Shi, "Phase Transformations in $\text{YBa}_2\text{Cu}_3\text{O}_{7-x}$ ", *Phy. Rev. B.*, Vol.39, No.7 (1989), pp. 4299-4305.

[21]. H. M. OBryan and P. K. Gallagher, "Kinetics of the Oxidation of $\text{Ba}_2\text{YCu}_3\text{O}_x$ Ceramics", *J. Mat. Res.*, 3(4), (1988), pp. 619-625.

[22]. G. V. Tendeloo, H. W. Zandbergen and S. Amelinckx, "The Vacancy Order-Disorder Transition in $\text{Ba}_2\text{YCu}_3\text{O}_{7-x}$ Observed By means of Electron Diffraction and Eletron Microscopy", *Soli. State Commu.* Vol63, No.7, (1987), pp. 603-606.

[23]. D. J. Eaglesham, C. J. Humphreys, W. J. Clegg, M. A. Harmer, N. MaN. Alford, and J. D. Birchall, "The Orthorhombic and Tetragonal Phases of $\text{YBa}_2\text{Cu}_3\text{O}_{9-x}$ ", *Ad. Ceram. Mat.* Vol.2, 3B, (1987), pp. 662-667.

[24]. Alario-Franco M. A., Capponi J. J., Chailout C. Chenavas J. and Marezio M., "Oxygen Vacancy Ordering in $\text{Ba}_2\text{YCu}_3\text{O}_{7-x}$, $0 \leq X \leq 1$, By Electron Diffraction Studies", *Mat. Res. Soc. Symp. Proc.* Vol.99, (1988), pp. 41-47.

[25]. Jorgensen, J. D., Hinks, M. A., Soderholmd, L., Volin, K. F., Hitterman, R. L., Grace, J. D. and Schuller Ivan K., "Oxygen Ordering and the Orthorhombic- to - Tetragonal Phase Transition in $\text{YBa}_2\text{Cu}_3\text{O}_{7-x}$ ", *Phys. Rev.*, B36, (1987), pp. 3608.

[26]. H. U. Krebs and R. Wordenweber, "Oxygen Diffusion and Phase Transformation in $\text{YBa}_2\text{Cu}_3\text{O}_x$ ", *J. Appl. Phys.*, 63(5), (1988), pp. 1642-1645.

- [27]. P. K. Gallagher, H. M. OBryan, S. A. Sunshine, D. W. Murphy, "Oxygen Stoichiometry in $\text{Ba}_2\text{YCu}_3\text{O}_x$ ", *Mat. Res. Bull.*, Vol.22, (1987), pp. 995-1006.
- [28]. I. W. Chen, S. Keating, C. Y. Keating, X. Wu, P. E. Reyes-Morel, and T. Y. Tien, "Superconductivity and the Tailoring of Lattice Parameters of the Compound $\text{YBa}_2\text{Cu}_3\text{O}_x$ ", *Ad. Ceram. Mat.*, Vol.2, 3B, (1987), pp. 457-470.
- [29]. J. M. Sanchez, F. Mejia-Lira, and J. L. Moran-Lopez, "Oxygen Order-Disorder Transition in the Superconductor $\text{YBa}_2\text{Cu}_3\text{O}_{6+x}$ ", *Phys. Rev. B.*, Vol.37, No.7, March (1988), pp. 3678-3680.
- [30]. D. Rios-Jara, C. Varea, A. Robledo, A. Huanosta, J. M. Dominguez, J. Omana, T. Akachi, and R. Escudero, "On the Twin Formation in Orthorhombic $\text{YBa}_2\text{Cu}_3\text{O}_{7-y}$ ", *Mat. Res. Soc. Symp. Proc.*, Vol.99, (1988), pp. 233-238.
- [31]. D. J. Werber, C. H. Chen, R. J. Cava, and B. Batlogg, "Diffraction Evidence for Oxygen-Vacancy Ordering in Annealed $\text{Ba}_2\text{YCu}_3\text{O}_{7-x}$ ($0.3 \leq X \leq 0.4$) Superconductors", *Phy. Rev. B.*, Vol.37, No.4, (1988), pp. 2317-2319.
- [32]. Sumio Iijima, T. Ichihashi, Y. Kubo and J. Tabuchi, "Twinning of High-Tc $\text{Ba}_2\text{YCu}_3\text{O}_{7-x}$ Oxides", *Jap. Jour. Appl. Phys.*, Vol.26, No.9, (1987), pp. L1478-L1481.
- [33]. S. Nakahara, T. Boone, M. F. Yan, G. J. Fisanick, and D. W. Johnson, Jr. "Defect Structure in $\text{Ba}_2\text{YCu}_3\text{O}_7$ ", *J. Appl. Phys.* 63(2), (1988), pp. 451-455.
- [34]. A. Brokman, "Shear Transformation and Twin Formation in $\text{YBa}_2\text{Cu}_3\text{O}_7$ ", *Soli. State Commu.* Vol.64, No.2, (1987), pp. 257-260.
- [35]. D. Shi, M. S. Boley, J. G. Chen, M. Tang, U. Welp, W. K. Kwok and B. Malecki, "Flux Pinning and Twin Boundaries in $\text{YBa}_2\text{Cu}_3\text{O}_{7-x}$ ", *Supercon. Sci. Technol.* 2, (1989), pp. 255-260.
- [36]. J. L. Modeau, C. Chailout, J. J. Capponi and M. Marezio, "Twinning in $\text{Ba}_2\text{YCu}_3\text{O}_{6+x}$ Single Crystals", *Soli. State Commu.*, 64(11), (1987), pp. 1349-1352.
- [37]. J. W. Ekin, "Transport Critical Current in Bulk Sintered $\text{YBa}_2\text{Cu}_3\text{O}_x$ and Possibilities for its Enhancement", *Ad. Ceram. Mat.*, Vol.2, 3B, (1987), pp. 586-591.
- [38]. P. Chaudhari, J. Mannhart, D. Dimos, C. C. Tsuei, J. Chi, M. M. Opryako, and M. Scheuermann, "Direct Measurement of the Superconducting Properties of Single Grain Boundaries in $\text{YBa}_2\text{Cu}_3\text{O}_{7-x}$ ", *Phy. Rev. Lett.*, Vol.60, (1988), pp. 1653-1656.
- [39]. S. Jin, R. C. Sherwood, T. H. Tiefel, R. B. van Dover, S. Nakahara and R. A. Fastnacht, "Critical Current Density and Fabrication of the Polycrystalline Y-Ba-Cu-O Superconductor", *Ceram. Supercon.* 2, Research Update, (1987), pp. 272-281.
- [40]. R. A. Camps, J. E. Evetts, B. A. Glowachi, S. B. Newcomb, and W. M. Stobbs, "The Role of Boundaries in the Superconducting Properties of Sintered $\text{YBa}_2\text{Cu}_3\text{O}_{7-x}$ ", *J. Mat. Res.*, Vol.2, No.6, (1987), pp. 750-756.

- [41]. T. M. Shaw, S. L. Shinde, D. Dimos, R. F. Cook, P. R. Duncombe, and C. Kroll, "The Effect of Grain Size on Microstructure and Stress Relaxation in Polycrystalline $\text{YBa}_2\text{Cu}_3\text{O}_{7-x}$ ", J. Mat. Res., Vol.4, No.2, (1989), pp. 248-256.
- [42]. L. Lynds, Francis Gralasso, F. Otter, B. R. Weinberger, J. I. Budnick, D. P. Yang, and M. Filipkowski, "Anisotropy in an Oriented $\text{Ba}_2\text{YCu}_3\text{O}_7$ Superconductor", J. Am. Ceram. Soc., 71(3), (1988), pp. C130-C132.
- [43]. Lawrence D. Fitch and Vernon L. Burdick, "Water Corrosion of $\text{YBa}_2\text{Cu}_3\text{O}_{7-x}$ Superconductors", J. Am. Ceram. Soc., 72(10), (1989), pp. 2020-2023.
- [44]. M. M. Garland, "Degradation of Y-Ba-Cu-O in a High-Humidity Environment", J. Mat. Res., 3(5), (1988), pp. 803-831.
- [45]. J. Dominec, L. Smrcka, P. Vasek, S. Geurten, O. Smrckova, D. Sykorova and B. Hajek, "Stability of $\text{YBa}_2\text{Cu}_3\text{O}_{7-y}$ Superconductor in Water", Solid State Comm., Vol. 65, No. 5, (1988), pp. 373-374.
- [46]. H. S. Horwitz, R. K. Bordia, R. B. Flippen and R. K. Johnson, "Effect of Ambient Atmosphere of $\text{YBa}_2\text{Cu}_3\text{O}_{7-y}$ ", Mat. Res. Soc. Symp. Proc., Vol.99, (1988), pp. 903-906.
- [47]. L. Zhang, J. Chen, H. M. Chan, and M. P. Harmer, "Formation of Grain-Boundary Carbon-Containing Phase During Annealing of $\text{YBa}_2\text{Cu}_3\text{O}_{6+x}$ ", J. Am. Ceram. Soc., 72(10), (1989), pp. 1997-2000.
- [48]. T. R. Dinger, T. K. Worthington, W. J. Gallagher, and R. L. Sandstorm, "Direct Observation of Electronic Anisotropy in Single-Crystal $\text{YBa}_2\text{Cu}_3\text{O}_{7-x}$ ", Phy. Rev. Lett. Vol.58, No. 25, (1987), pp. 2687-2690.
- [49]. L. C. Stearns, M. D. Vaudin, C. P. Ostertag, J. E. Blendell, and E. R. Fuller, Jr., "Texture Development in $\text{Ba}_2\text{Cu}_3\text{O}_{6+x}$ Through Sinter-Forging", Ceram. Supercond. 2, Res. Update, (1988), pp. 315-322.
- [50]. J. M. Tranquada, A. I. Goldman, A. R. Moodenbaugh, G. Shirane, S. K. Sinha, A. J. Jacobson, and J. T. Lewandowski, "Observation of Alignment of Superconducting $\text{YBa}_2\text{Cu}_3\text{O}_7$ Particles in a Magnetic Field Using Neutron Diffraction", Phy. Rev. B, Vol.37, No.1, (1988), pp. 519-521.
- [51]. K. Sadananda, A. K. Sinch, M. A. Iman, M. Osofsky, V. Le Tourneau, and L. E. Richards, "Effect of Hot Isostatic Pressing on $\text{RBa}_2\text{Cu}_3\text{O}_7$ Superconductors", Ad. Ceram. Mat., 3(5), (1988), pp. 524-536.
- [52]. Siu-Wai Chan, D. M. Hwang, R. Ramesh, S. M. Sampere, L. Nazar, R. Gerhardt, and P. Prouna, "Study of $\text{YBa}_2\text{Cu}_3\text{O}_{7-x}$ Thin Films Grown on Single Crystal SrTiO_3 : Not All High Angle Grain Boundaries Destroy J_c ", High Tc Supercon. Thin Films, AIP Confere. Proc, No.200, (1990), pp. 172.
- [53]. S. Jin, T. H. Tiefel, R. C. Sherwood, M. E. Davis, R. B. Van Dover, G. W. Kammlott, R. A. Fastnacht, and H. D. Keith, "High Critical Currents in Y-Ba-Cu-O

Superconductors", Appl. Phys. Lett. 52(24), (1988), pp. 2074-2076.

[54]. L. Zhang, H. M. Chan, and M. P. Harmer, "Seeding Induced Aligned Microstructures in $\text{YBa}_2\text{Cu}_3\text{O}_{6+x}$ ", Mat. Res. Soc. Symp. Proc., Vol. 157, (1989).

[55]. K. Salama, V. Selvamanickam, L. Gao, and K. Sun, "High Current Density in Bulk $\text{YBa}_2\text{Cu}_3\text{O}_x$ Superconductor", Appl. Phys. Lett. 54(23), (1989), pp. 2352-2354.

[56]. D. R. Clarke, T. M. Shaw and D. Dimos, "Issues in the Processing of Cuprate Ceramic Superconductors", J. Am. Ceram. Soc. 72(7), (1989), pp. 1103-1113.

[57]. T. Aselage and K. Keefer, "Liquidus Relations in Y-Ba-Cu Oxides", J. Mat. Res. 3(6), (1988), pp. 1279-1291.

[58]. R. S. Roth, C. J. Rawn, F. Beech, J. D. Whitler, J. O. Anderson, "Phase Equilibria in the System Ba-Y-Cu-O- CO_2 in Air", Ceram. Supercon. 2, Research Update, (1988), pp. 13-26.

[59]. A. F. Hepp, J. R. Gaier, G. A. Landis, and S. G. Bailey, "Crystallite Alignment of Polycrystalline $\text{Ba}_2\text{YCu}_3\text{O}_{7-x}$ ", Ceram. Supercon. 2, Research Update, (1988), pp. 356-366.

Vita

LIJIE ZHANG, daughter of YUNCHONG ZHANG and BINGZHEN HU, was born in CHANGCHUN, JILING, CHINA, on April 8, 1956. She graduated from Tsinghua University, CHINA in 1982, with a Bachelor of Engineering degree in Materials Engineering. After graduation, she worked on Ceramic Materials at the Institute of Materials Research, China. In 1986, she came to the United States, and since 1987, she has studied at Lehigh University. This thesis was done while she worked as a visiting scientist, supported by the Lehigh University Consortium for Superconducting Ceramics. During the course of this work, she gave birth to her daughter Anbai on April 10, 1990. Upon completion of her Master's Degree, she will begin working as a Research Associate at Lehigh on grain alignment in ceramic superconductors.